remote sensing

MDPI

Review

A Review of High-Sensitivity Tracking Techniques for Satellite Navigation Signals

Zhiqiang Gong [1,2], Honglei Lin [1,2,*], Zhe Liu [1,2], Zengjun Liu [1,2], Long Huang [1,2] and Gang Ou [1,2]

[1] College of Electronic Science and Technology, National University of Defense Technology, Changsha 410073, China; zhiqiang200201@163.com (Z.G.); liuzhe@nudt.edu.cn (Z.L.); liuzengjun@nudt.edu.cn (Z.L.); huanglong@nudt.edu.cn (L.H.); ougang@nudt.edu.cn (G.O.)
[2] National Key Laboratory for Positioning, Navigation and Timing Technology, Changsha 410073, China
* Correspondence: linhonglei@nudt.edu.cn

Abstract: With the increasing demand for high-sensitivity signal tracking in complex environments, GNSS receiver technologies have continuously evolved in both architecture and algorithmic design. This paper presents a systematic review of the development of high-sensitivity tracking techniques, with a focus on the transition from closed-loop to open-loop, hybrid, and deeply integrated architectures. Key strategies—such as coherent integration time extension, discriminator and loop filter optimization, vector tracking (VT), and Direct Position Estimation (DPE) are evaluated in the context of weak signal scenarios. To address the limitations of existing methods, including strong dependence on filter models, oscillator instability, and computational complexity, this study also outlines future research directions, including (1) integrating deep learning techniques into filter structures to enhance adaptability and robustness; (2) developing multi-channel collaborative estimation schemes to mitigate oscillator noise in weak signal environments; and (3) designing low-complexity open-loop tracking approximations to align with hardware resource constraints. Thus, enhancing the necessity of navigation continuity and robustness under low-signal-to-noise-ratio (SNR) conditions.

Keywords: high-sensitivity tracking; closed-loop tracking; open-loop tracking; direct position estimation (DPE)

check for updates

Academic Editor: Antonio Miguel Ruiz Armenteros

Received: 17 March 2025
Revised: 2 May 2025
Accepted: 8 May 2025
Published: 14 May 2025

Citation: Gong, Z.; Lin, H.; Liu, Z.; Liu, Z.; Huang, L.; Ou, G. A Review of High-Sensitivity Tracking Techniques for Satellite Navigation Signals. *Remote Sens.* **2025**, *17*, 1713. https://doi.org/10.3390/rs17101713

Copyright: © 2025 by the authors. Licensee MDPI, Basel, Switzerland. This article is an open access article distributed under the terms and conditions of the Creative Commons Attribution (CC BY) license (https://creativecommons.org/licenses/by/4.0/).

1. Introduction

With improvements in living standards and advancements in science and technology, the demand for accurate positioning in daily life has increased significantly. This has driven the development of various positioning technologies, including the Global Navigation Satellite System (GNSS), Bluetooth, Ultra-Wideband (UWB), and Wi-Fi [1]. Among these, GNSS stands out due to its wide coverage and diverse range of applications [2]. Since its successful introduction, GNSS has been deployed extensively in various scenarios [3], and the rise of automation and intelligent systems has expanded its applications even further. Technological advancements such as autonomous driving and Unmanned Aerial Vehicle (UAV) navigation have heightened the demand for Positioning, Navigation, and Timing (PNT) solutions capable of providing high accuracy, even in challenging environments like urban canyons and indoor spaces [4].

Currently, standard GNSS technology meets most positioning needs under Line-of-Sight (LOS) conditions. However, it faces significant limitations in complex environments, such as urban canyons and indoor spaces. The primary factor affecting GNSS performance in these settings is the signal-to-noise ratio (SNR), which is typically 10 to 30 dB lower than

in open areas [5]. As a result, standard GNSS technology struggles to deliver sufficient positioning accuracy and reliability in these environments [6].

To address these challenges, the development of high-sensitivity positioning technologies is essential. These technologies are designed to provide precise and reliable positioning information even in low SNR and complex environments [7]. High-sensitivity positioning is particularly crucial in applications that require high accuracy and reliability. For smart unmanned systems, such as autonomous vehicles and drones, reliable positioning is vital for real-time decision-making, path planning, and mission execution. High-sensitivity positioning ensures safe navigation and operation in challenging environments like cities, forests, and mountains.

Furthermore, the demand for high-sensitivity positioning is becoming more urgent with the advent of miniaturized, consumer-grade smart wearable devices [8]. Compact antenna designs, with their negative gain and high front-end loss, often result in low equivalent carrier-to-noise ratios, thus compromising signal reception quality. Additionally, for other smart mobile devices, such as smartphones, high-sensitivity positioning can significantly improve the accuracy of indoor navigation, location-based services, and augmented reality applications [9].

A key component in achieving high-sensitivity positioning is the effective tracking of navigation signals [10]. The satellite signal tracking module consists of two main components: carrier tracking and pseudo-code tracking. Notably, the sensitivity of the code tracking loop is typically 5 to 9 dB higher than that of the carrier tracking loop, and the frequency change rate of the pseudo-code is only 1/1000th of that of the carrier frequency [5]. In complex environments, the sensitivity of carrier tracking becomes the decisive factor in determining the overall tracking performance of the receiver.

Although the importance of high-sensitivity tracking techniques is increasingly recognized, the existing literature still lacks a systematic and structured review of this field. To address this gap, this paper makes the following key contributions. First, it proposes a unified classification framework that systematically categorizes high-sensitivity GNSS signal tracking techniques into four major types: scalar tracking, vector tracking, conventional open-loop processing, and Direct Position Estimation (DPE). This classification clearly delineates their fundamental principles and applicable scenarios. Second, this paper provides an in-depth analysis of mainstream tracking technologies and sensitivity enhancement strategies, focusing on techniques such as coherent integration time extension, oscillator noise modeling and mitigation, and advanced filtering algorithms. Finally, this paper outlines emerging research directions, including integrating deep learning techniques into filter structures to enhance adaptability and robustness in dynamic environments; developing multi-channel collaborative estimation schemes for oscillator noise, incorporating external signal data such as 4G/5G communication signals to improve system performance; and designing low-complexity approximations for open-loop tracking to better align with hardware resource constraints while maintaining sensitivity and dynamic performance.Collectively, these contributions offer theoretical guidance for the design and optimization of high-sensitivity GNSS receivers and provide a clear roadmap for future research in this field.

2. Methods

2.1. Tracking Methods

Tracking of satellite signals is a fundamental function of Global Navigation Satellite System (GNSS) receivers and is essential for ensuring accurate and reliable positioning. These tracking techniques can be systematically categorized based on their feedback structure and utilization of auxiliary information.

Broadly, carrier tracking falls into two primary categories: closed-loop tracking and open-loop tracking, distinguished by whether a real-time feedback mechanism is employed [11]. Closed-loop tracking is the traditional method widely adopted due to its low computational complexity. However, it imposes a stringent stability constraint: the product of coherent integration time and loop noise bandwidth must remain below 0.5 [12]. This limitation becomes critical in dynamic or weak-signal scenarios, where long integration times and wider bandwidths are required—potentially leading to loop instability.

Within closed-loop architectures, two subtypes are commonly used: scalar tracking and vector tracking (VT) [13]. Scalar tracking treats each satellite channel independently, estimating propagation delays without leveraging inter-satellite geometry. While simple, this approach does not exploit the spatial relationships between signals, which limits its performance in complex environments.

In contrast, vector tracking employs a shared navigation filter that fuses measurements across all channels [14]. The navigation solution, obtained from all satellite observations, generates synchronized feedback for each channel, improving tracking robustness and accuracy—particularly under degraded signal conditions.

Compared to closed-loop methods, open-loop tracking imposes higher computational demands but offers critical advantages. By employing feedforward estimation instead of feedback loops, open-loop tracking maintains better signal observability, especially in high-dynamic scenarios where Doppler effects cause rapid frequency variations [15]. This architecture enables broader search spaces and faster re-acquisition of signals following fading or interruption, as it can initiate estimation as soon as new samples arrive [16].

Moreover, open-loop systems inherently avoid the stability issues associated with feedback-based filters [17]. Like closed-loop techniques, open-loop tracking can be classified into traditional open-loop tracking, which emphasizes feature extraction, and Direct Position Estimation (DPE), which estimates the receiver's position directly using the signal's geometric structure.

Table 1 provides a structured comparison of the major GNSS signal tracking methods introduced above. It summarizes their core concepts, strengths, limitations, and representative references. This overview helps clarify the evolution of tracking techniques and highlights the trade-offs among different architectures in terms of complexity, robustness, and implementation feasibility.

Another dimension of classification concerns whether external assistance is used. Standalone GNSS receivers rely solely on internal signal processing, whereas Assisted GNSS (A-GNSS) receivers integrate external sensor data—such as inertial measurement units (IMUs) or gyroscopes—to improve tracking performance, especially in signal-denied environments [13,18].

A summary of these tracking methods and their interrelationships is presented in Figure 1. This paper adopts the aforementioned classification as a framework to review recent advances in GNSS signal tracking, analyze their respective advantages and limitations across application scenarios, and identify promising directions for future research.

2.2. Scalar Tracking

Scalar tracking is the most traditional method of closed-loop tracking, and its block diagram is shown in Figure 2. This tracking loop consists of four main components: a correlation module, a discriminator module, a loop filter, and a voltage-controlled oscillator.

Table 1. Comparison of major GNSS signal tracking methods.

Tracking Method	Core Concept	Advantages	Limitations	Representative References
Scalar Tracking	Each satellite channel is tracked independently without exploiting inter-satellite geometry.	Simple structure; low computational cost.	Poor performance in dynamic or degraded environments; no channel cooperation.	Zhodzishsky, M. (1998) [19], Spilker Jr, J. (1996) [13], Pany, T. (2005) [20], Lian, P. (2005) [21], Ziedan, N. I. (2004) [10], Ren, T. (2012) [22], Curran, J. T. (2012) [23], Sun, Z. (2013) [24], Guo, W. (2014) [25], Yan, K. (2016) [11], Chen, S. (2017) [26], Li, J. (2018) [27], Feng, X. (2023) [12]
Vector Tracking	Navigation solution derived from all channels jointly feeds back into all loops, utilizing inter-channel geometric relationships.	Robust tracking in weak signal scenarios; better accuracy.	Complex navigation filter; sensitive to modeling errors.	Copps, D. B. (1980) [28], Lashley, M. (2007) [29], Lashley, M. (2009) [30], Lashley, M. (2009) [31], Lashley, M. (2010) [32], Henkel, P. (2009) [33], Chen, Q. (2014) [34], Peng, S. (2012) [35], Yang, H. (2021) [36], Farhad, M. (2021) [37], Mou, M. (2021) [14], Liu, W. (2022) [38], Marcal, J. (2016) [39], Lin, H. (2017) [40], Chen, Q. (2018) [41]
Open-Loop Tracking	Signal parameters are estimated through feedforward processing without feedback loops.	High observability; robust re-acquisition in fading.	High computational complexity; less suitable for real-time use.	Van Graas, F. (2005) [42], Anyaegbu, E. (2006) [43], Yan, K. (2016) [11], Tahir, M. (2012) [44], Jin, T. (2020) [45], Wu, C. (2022) [46], Stienne, G. (2012) [47], Closas, P. (2007) [48], Tahir, M. (2012) [49]
Direct Position Estimation	Jointly estimates position directly from raw signals without intermediate synchronization steps.	High positioning accuracy; bypasses code/carrier synchronization.	Computationally expensive; limited practical deployment.	Closas, P. (2007) [48], Closas, P. (2008) [50], Closas, P. (2009) [51], Closas, P. (2010) [52], Closas, P. (2017) [53], Amar, A. (2008) [54], Ramesh Kumar, A. (2015) [55], Ng, Y. (2016) [56], Chu, A. H.-P. (2019) [57]

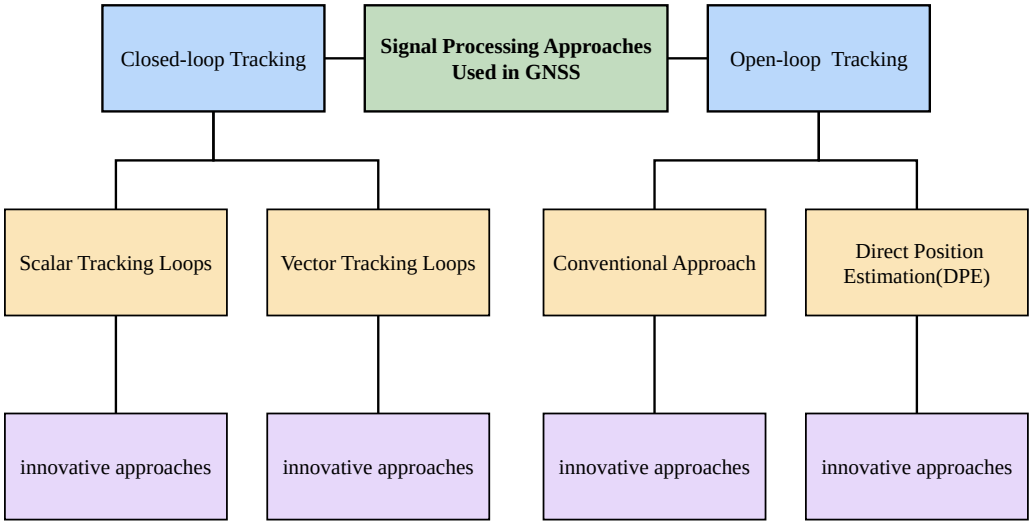


Figure 1. Overview of satellite signal tracking techniques in GNSS receivers.

The open-loop transfer function is defined as

$$G_{OL}(s) = \frac{K_d K_o F(s)}{s} \tag{1}$$

The closed-loop transfer function is

$$H_{CL}(s) = \frac{G_{OL}(s)}{1 + G_{OL}(s)} = \frac{K_d K_o F(s)}{s + K_d K_o F(s)} \tag{2}$$

The error transfer function is

$$E(s) = \frac{1}{1 + G_{OL}(s)} = \frac{s}{s + K_d K_o F(s)} \tag{3}$$

where K_d is the phase discriminator gain, K_o is the voltage-controlled oscillator gain, and $F(s)$ is the loop filter transfer function.

For a second-order tracking system, the loop filter $F(s)$ can be explicitly expressed as

$$F(s) = \frac{\tau_2 s + 1}{\tau_1 s} \tag{4}$$

where τ_1 is the integrator time constant of the filter, and τ_2 is the zero time constant of the filter.

For commonly used parameters in satellite signal tracking, the inherent frequency ω_n and damping factor ζ of this are

$$\omega_n = \sqrt{\frac{K_d K_o}{\tau_1}} = \sqrt{K_d K_o K_2} \tag{5}$$

$$\zeta = \frac{\tau_2}{2}\sqrt{\frac{K_d K_o}{\tau_1}} = \frac{\tau_2 \omega_n}{2} = \frac{K_1}{2}\sqrt{\frac{K_d K_o}{K_2}} \tag{6}$$

Substituting these parameters into the closed-loop transfer function expression, the second-order tracking system transfer function can be simplified as:

$$H(s) = \frac{2\zeta\omega_n s + \omega_n^2}{s^2 + 2\zeta\omega_n s + \omega_n^2} \tag{7}$$

To enhance the tracking sensitivity of the scalar tracking loop, researchers have proposed three primary approaches: (1) improving the SNR by extending the coherent integration time, (2) enhancing the discriminator's estimation accuracy to more precisely capture signal features, and (3) optimizing the loop filter to improve overall signal processing performance.

As Assisted GNSS (A-GNSS) has already been integrated into some of these innovations, the combination of scalar tracking with A-GNSS is not discussed separately in this section.

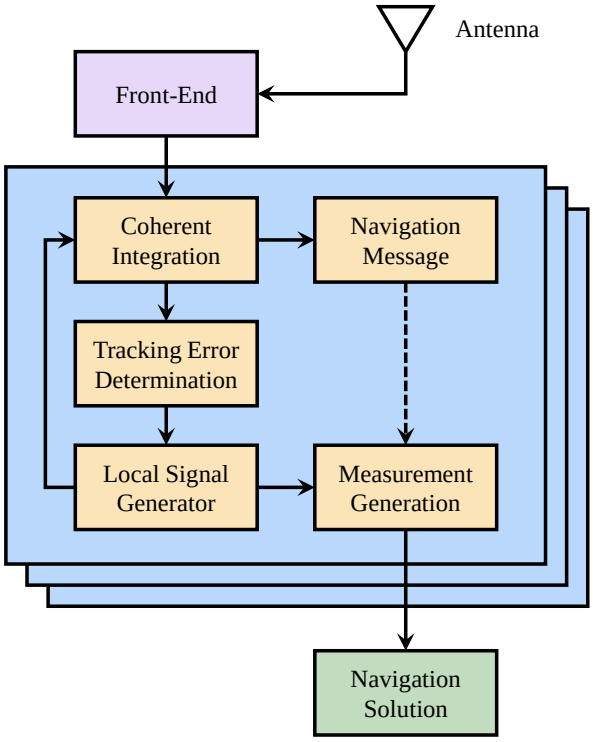


Figure 2. Methods of the scalar tracking loop.

2.2.1. Extending Coherent Integration Time

In GNSS receivers, extending the coherent integration time is a key strategy for improving tracking sensitivity. It also helps mitigate undesirable effects such as multipath and Non-Line-of-Sight (NLOS) propagation. However, extending the coherent integration time introduces three major challenges: navigation bit flips, receiver dynamics, and oscillator instability [58].

For standalone GNSS receivers, Ren first proposed using Maximum-Likelihood (ML) algorithms to extend coherent integration by performing data erasure after bit synchronization [22]. Daniele Borio later achieved the integration of multiple 20 ms coherent integrations using non-coherent integration combined with a memory discriminator, which effectively mitigates the effects of data bit flipping [59,60]. When a reference base station is available, A-GNSS can be used to eliminate the effects of data bit flipping [18]. Furthermore, for modern signal regimes such as B1c and L5, tracking these signals is not impacted by navigation data bit flipping, as the guiding frequency signals are modulated into known secondary codes [61,62].

To address the effects of receiver dynamics, inertial navigation systems (INSs) are commonly used to assist GNSS receivers [20]. The concept of deep combining was first introduced by Gustafson at Draper Laboratories in 1996, describing a combinatorial navigation method for extended code tracking loops. Following this, Draper Laboratories conducted extensive research on ultra-tight combining in a collaborative military project [63]. This led

to the development of the theoretical foundation for ultra-tight combining, which involves assisting the scalar tracking loop of the GNSS receiver with INS data. The architecture of a scalar ultra-tight combined tracking loop assisted by INS is shown in Figure 3.

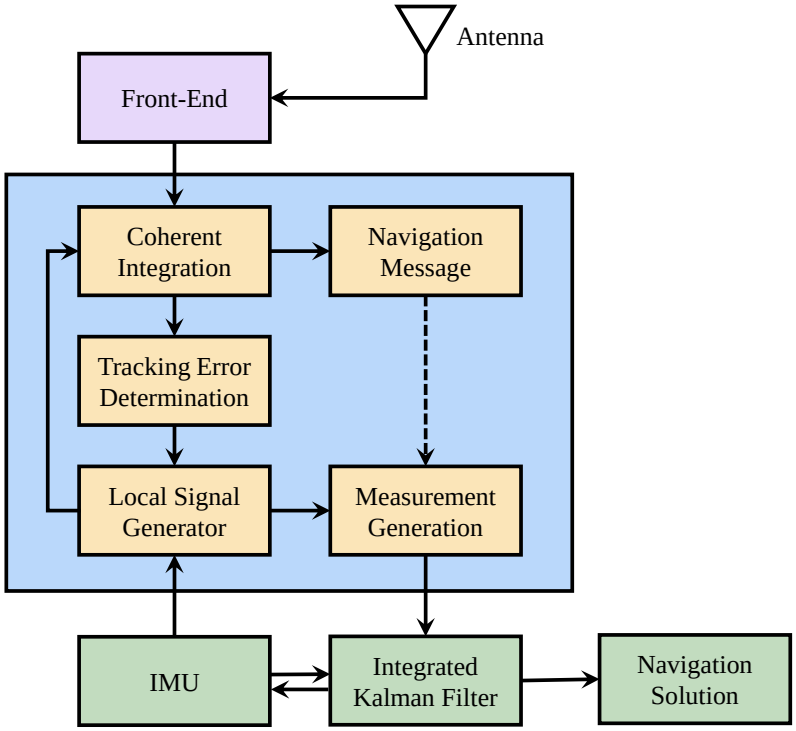


Figure 3. Methods of the INS-assisted scalar ultra-tight combined tracking loop.

Since the beginning of the 21st century, ultra-tight integration navigation technology has developed rapidly. Researchers have demonstrated that GNSS carrier loops can operate effectively under quasi-static conditions with the assistance of INS [64–66]. Niu quantitatively assessed the negative impact of inertial assistance for different types of INS by modeling phase-locked loop (PLL) in a deeply integrated Global Positioning System(GPS)/INS system using scalar tracking. Their results show that the carrier phase tracking errors are below 1.2 degrees for Micro-Electro-Mechanical System (MEMS) IMUs and below 0.8 degrees for tactical IMUs, which are much smaller than the inherent receiver errors. This indicates that even low-cost MEMS IMUs can assist in signal tracking, while tactical-grade IMUs provide higher-quality auxiliary information [67].

Zhang et al. demonstrated through real-world, highly dynamic field tests that the carrier phase error of a MEMS IMU-assisted PLL is nearly identical to that under static conditions [66]. Ultra-tight GNSS/INS integration has been validated as an effective method for mitigating receiver dynamics during long coherent integrations [64,66,68].

Oscillator phase noise can be categorized into long-term and short-term effects. Long-term effects include deterministic phase and frequency trends, such as frequency bias and linear frequency drift, while short-term effects involve random phase and frequency fluctuations [23]. The process of oscillator phase noise can be described as follows [23,69]:

$$\Psi_{n+1}(t) = 2\pi f_0 t + \sum_{i=2}^{N} \frac{2\pi \delta f_{i-1}}{i!} t^i + \psi(t) = \Psi_n(t) \tag{8}$$

where f_0 and δf_i represent the constant average frequency and the i-th order frequency drift of the oscillator, respectively [69]. The short-term effect, $\psi(t)$, is modeled as a zero-mean stochastic process. Any non-zero average phase noise can be absorbed into the system

drift. Long-term effects are typically not a concern for carrier tracking, as any frequency deviations can be absorbed into the satellite Doppler estimate, and higher-order drifts are negligible compared to the satellite Doppler drift. Therefore, long-term effects are often ignored, and the short-term random effects of the oscillator are the primary factors affecting the receiver [23].

The impact of oscillator instability on coherent integration time has been extensively studied. Consumer-grade oscillators are typically limited to coherent integration times of up to 500 ms, while ultra-stable oscillators can support integration times of several seconds, which is critical for high-sensitivity GNSS applications [23,70–72]. However, due to cost constraints, consumer-level GNSS receivers cannot afford the high-performance ultra-stable oscillators required for extended integration times. As a result, PLLs must be carefully designed to mitigate the instability of the local oscillator [73].

Currently, techniques to address GNSS receiver oscillator instability are broadly classified into two categories: difference-based methods and estimation-based methods. Difference-based methods were first introduced by Pany and eliminate common clock errors by performing single and double differences at the correlator level between the rover and the base station. This technique achieves coherent integration times of up to 100 s for static applications, with a single-channel carrier tracking sensitivity of $-14\,\mathrm{dB}\cdot\mathrm{Hz}$ and an indoor positioning accuracy of 1 m [74,75].

Curran achieved more robust tracking by appropriately modeling oscillator noise and using the Wiener filter as a causal filter applied to the carrier phase tracking problem [23]. Similarly, Chen utilized Kalman filtering algorithms to track oscillator noise, thereby improving carrier phase tracking [26]. Zhodzishsky proposed a different approach, simultaneously estimating oscillator noise using multiple channels by tracking receiver position errors and oscillator biases with four filters [19]. Building on this, Zhuo developed a carrier phase tracking method that estimates oscillator phase noise using information from multiple correlators [76].

Subsequently, Zhodzishsky introduced the quartz phase-locked loop (QLL) system, which optimizes the tracking loop into a common loop and multiple individual loops. This approach addresses the problem of oscillator instability caused by receiver vibrations, thereby improving the vibration immunity of GNSS receivers [77]. Xin further advanced this approach by proposing a long, coherent integration method for improved carrier phase tracking. This method uses a multi-channel cooperative loop to track the receiver's oscillator error and combines it with a local loop for ultra-long coherent integration cycles. However, a key limitation is that strong satellite signals are required to achieve long coherent integration for weak satellite signals [12].

In summary, while there are mature solutions for problems like data code flipping and user dynamics when extending coherent integration time, the issue of oscillator instability remains an ongoing challenge. Although various methods have been proposed to address oscillator instability, each has its limitations, and a comprehensive solution is yet to be found. As a result, oscillator instability continues to be a primary focus of future high-sensitivity GNSS tracking research.

Table 2 summarizes the major techniques proposed for extending coherent integration time, including their strengths, challenges, and representative works. This comparative overview highlights the evolving landscape of high-sensitivity GNSS tracking innovations.

Table 2. Summary of techniques for extending coherent integration time.

Technique	Advantages	Challenges	Representative References
Maximum Likelihood	Extends coherent integration by performing data erasure after bit synchronization.	Navigation bit flips; computational complexity.	Ren, T. (2012) [22]
Non-Coherent Integration	Combines multiple 20 ms coherent integrations using a memory discriminator.	Computational complexity; synchronization between different channels.	Borio, D. (2009) [59], Borio, D. (2009) [60]
Assisted GNSS	Eliminates the effects of data bit flipping using reference base stations.	Requires a reference station; limited by signal availability.	Van Diggelen, F. (2009) [18]
Deep Combining with INS	Enhances GNSS tracking by combining with inertial navigation systems to mitigate receiver dynamics.	High cost of INS; requires sophisticated integration.	Pany, T. (2005) [20], Pany, T. (2009) [64]
Wiener Filtering	Robustly tracks the carrier phase by modeling oscillator noise.	Complexity of filter design; requires high-quality oscillators.	Curran, J. T. (2012) [23]
Kalman Filtering	Uses Kalman filters to track oscillator noise and improve carrier phase tracking accuracy.	High computational load; needs accurate noise models.	Chen, S. (2017) [26], Zhodzishsky, M. (1998) [19]
Quartz Phase-Locked Loop	Optimizes tracking loops into a common loop and multiple individual loops to improve stability.	Receiver vibration can still impact performance; requires strong signals.	Zhodzishsky, M. (2020) [77]
Long Coherent Integration	Uses multi-channel cooperative loops to track oscillator error for ultra-long coherent integration cycles.	Requires strong satellite signals; high complexity.	Feng, X. (2023) [12]

2.2.2. Optimizing the Discriminator

In the pursuit of improving GNSS receiver discriminator sensitivity, past research has predominantly focused on Frequency-Locked Loop (FLL) discriminators, which include ML frequency estimation, differential amplitude (DA) discriminators, and FFT-based discriminators. Daniele Borio was the first to propose the use of ML estimation for frequency estimation of coherent integration signals. This approach, based on the Discrete-Time Fourier Transform (DTFT), enables effective frequency estimation using ML principles [78].

The DA discriminator was first introduced by Wenfei Guo, who used multiple Numerically Controlled Oscillators (NCOs) to replicate the same structure as the early delay, enabling frequency discrimination [25]. Building on this, Ji Li proposed a memory discriminator that combines the DA discriminator with a moving window function. This modification improves Doppler estimation quality by reducing measurement variance, minimizing noise effects, and enhancing tracking performance [27].

FFT operations provide a more efficient way to obtain linear measurements and offer lower tracking SNR thresholds compared to conventional discriminators [79]. As a result, FFT-based frequency tracking has become an increasingly powerful solution [15,78,80–82]. However, due to the high computational complexity of FFT, most studies have focused on its use in open-loop tracking, with fewer applications in scalar tracking.

The use of FFT in closed-loop tracking was first introduced by Kunlun Yan, who proposed using FFT to process the in-phase and quadrature (I/Q) coherent integration results in closed-loop tracking, reducing computational complexity and marking its application in scalar tracking [11]. This approach was further extended by incorporating INS to improve tracking sensitivity [83]. Additionally, Yang introduced an FFT-based tracking method for GPS code phase and carrier frequency [80], and Xinlong Wang implemented an FFT-based dynamic segmentation tracking loop [84].

A key feature of these methods is their deviation from the standard coherent integration signals for frequency discrimination, instead using multiband or early-delayed coherent integration signals. However, for receiver ranging in these methods, pseudo-code ranging is typically used, which is less accurate than carrier phase ranging. Therefore, optimizing estimators for PLLs remains a crucial research area, particularly with respect to frequency estimators using multiband or early-delayed coherent integration signals.

Table 3 provides a comparative summary of key discriminator optimization techniques discussed above. It highlights their respective strengths, challenges, and representative works in GNSS tracking research.

Table 3. Comparison of discriminator optimization techniques in GNSS receivers.

Discriminator Type	Advantages	Limitations	Representative References
Maximum Likelihood	High estimation accuracy using DTFT; effective in low SNR conditions.	Computational complexity; sensitive to bit flips.	Borio, D. (2008) [78]
Differential Amplitude	Uses multiple NCOs; straightforward structure.	Performance degrades in dynamic environments.	Guo, W. (2014) [25], Li, J. (2018) [27]
FFT-Based Estimation	Applies FFT on I/Q coherent integration results in closed-loop tracking; enables real-time processing.	Implementation complexity; less explored in the literature.	Yan, K. (2016) [11], Yan, K. (2017) [83], Wang, X. (2015) [84], Van Graas, F. (2009) [15], Borio, D. (2008) [78], Ba, X. (2009) [82]
Multiband/Early Delayed	Allows higher frequency resolution; applicable to dynamic environments.	Pseudorange accuracy lower than carrier phase; estimator design more complex.	Yang, C. (2003) [80], Wang, X. (2015) [84]

2.2.3. Optimizing the Loop Filter

Optimizing the loop filter is a crucial research area for enhancing the tracking sensitivity of GNSS receivers. This improvement can be categorized into two main approaches: the Wiener filter and the Kalman Filter (KF). Wiener filters are widely used due to their effectiveness in mitigating thermal and oscillator noise within the loop. As demonstrated in Curran's work, designs incorporating Wiener filters offer superior tracking performance compared to conventional PLL designs [23].

KF optimization can be further divided into two approaches: the linear KF, which treats discriminator outputs as observations, and the Extended Kalman Filter (EKF), which processes outputs from the I and Q correlators with non-linear observations. The block diagrams illustrating the flow in both approaches are shown in Figure 4.

The first approach, shown in the left panel of Figure 4, combines the baseband I and Q values to generate signal parameter error values via a nonlinear discriminator function, which are then processed using a KF. The advantage of this approach lies in the simplicity of its design matrix, as the discriminator output is directly used as the measurement residual. However, a major drawback is that the covariance of the measurement noise is no longer white Gaussian, primarily because the nonlinear discriminator function causes a loss of the white Gaussian noise properties [85]. Nonetheless, by assuming a quasi-Gaussian distribution, a robust implementation can still be achieved.

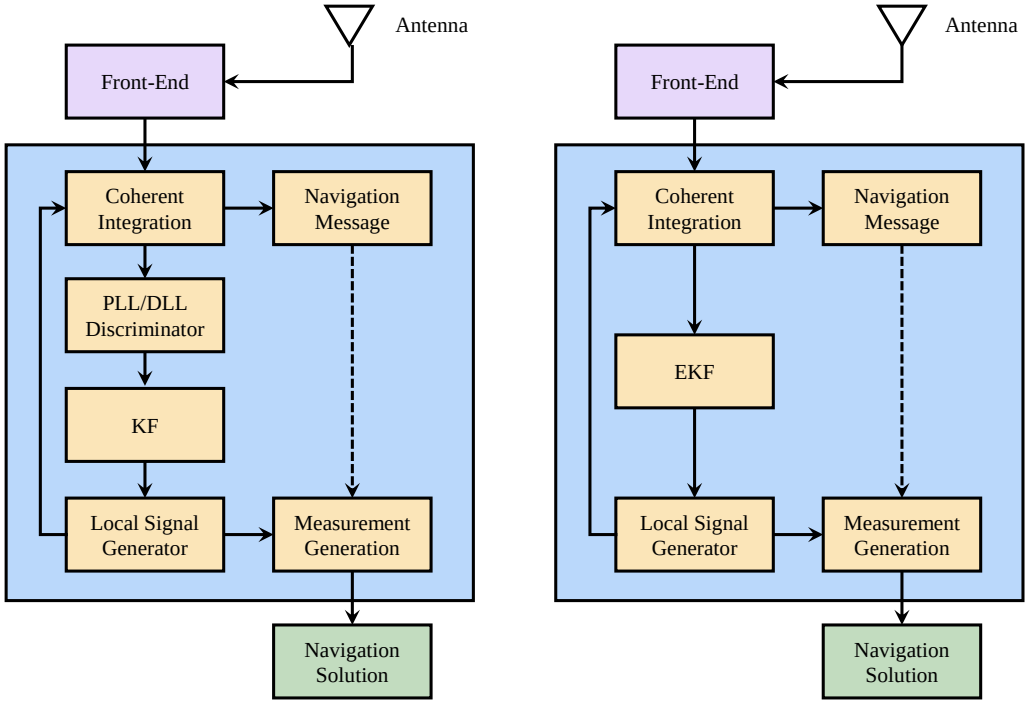


Figure 4. Methods of KF and EKF optimization.

The carrier tracking loop based on the KF algorithm is modeled as follows [21]:

$$\begin{bmatrix} \theta_{e,k+1} \\ f_{d,k+1} \\ f_{a,k+1} \end{bmatrix} = \begin{bmatrix} 1 & \Delta t & \frac{\Delta t^2}{2} \\ 0 & 1 & \Delta t \\ 0 & 0 & 1 \end{bmatrix} \begin{bmatrix} \theta_{e,k} \\ f_{d,k} \\ f_{a,k} \end{bmatrix} - \begin{bmatrix} \Delta t \\ 0 \\ 0 \end{bmatrix} f_{d,k}^{NCO} + W_n \tag{9}$$

where $\theta_{e,k}$ represents the carrier phase error between the input signal and the NCO output, $f_{d,k}$ is the Doppler frequency in the input signal, and $f_{a,k}$ is the rate of change of the Doppler frequency due to acceleration along the Line-of-Sight (LOS) direction between the satellite and the receiver. $f_{d,k-1}^{NCO}$ is the Doppler frequency replicated by the NCO, and Δt is the updating period (or pre-integration time). $W_n = \begin{bmatrix} W_\theta & W_d & W_a \end{bmatrix}^T$ is the noise vector, consisting of a sequence of discrete Gaussian white noise components, with covariance matrix Q.

The system matrix and spectral intensity in continuous time are given by [21]:

$$\Phi_{k+1,k} = \begin{bmatrix} 1 & \Delta t & \frac{\Delta t^2}{2} \\ 0 & 1 & \Delta t \\ 0 & 0 & 1 \end{bmatrix}, \quad Q_c = \begin{bmatrix} Q_\theta & 0 & 0 \\ 0 & Q_d & 0 \\ 0 & 0 & Q_a \end{bmatrix} \tag{10}$$

where Q_θ represents the receiver clock phase bias, Q_d corresponds to the receiver clock frequency drift, and Q_a is caused by the acceleration along the LOS direction [21].

$$\begin{aligned} Q &= \int_0^{\Delta t} \Phi_{k+1,k} Q_c \Phi_{k+1,k}^T \, dt \\ &= Q_\theta \begin{bmatrix} \Delta t & 0 & 0 \\ 0 & 0 & 0 \\ 0 & 0 & 0 \end{bmatrix} + Q_d \begin{bmatrix} \frac{\Delta t^3}{3} & \frac{\Delta t^2}{2} & 0 \\ \frac{\Delta t^2}{2} & \Delta t & 0 \\ 0 & 0 & 0 \end{bmatrix} + Q_a \begin{bmatrix} \frac{\Delta t^5}{20} & \frac{\Delta t^4}{8} & \frac{\Delta t^3}{6} \\ \frac{\Delta t^4}{8} & \frac{\Delta t^3}{3} & \frac{\Delta t^2}{2} \\ \frac{\Delta t^3}{6} & \frac{\Delta t^2}{2} & \Delta t \end{bmatrix} \end{aligned} \tag{11}$$

The measurement equation is [21]:

$$\theta_{e,k}^{\text{mea}} = \begin{bmatrix} 1 & \frac{\Delta t}{2} & \frac{\Delta t^2}{6} \end{bmatrix} \begin{bmatrix} \theta_{e,k-1} \\ f_{d,k-1} \\ f_{a,k-1} \end{bmatrix} - \frac{\Delta t}{2} f_{d,k-1}^{NCO} + V_k \tag{12}$$

where $\theta_{e,k-1}^{\text{mea}}$ is the measured value of the carrier phase error, and V_{k-1} is a Gaussian white noise sequence.

Patrick Henkel and Lashley et al. used the KF algorithm as an alternative to the conventional loop filter and optimized the KF algorithm's parameters using a control method. They mathematically demonstrated the equivalence of the KF-based tracking loop and the conventional third-order PLL [31,33,35]. Building on this, Wei Liu compared the KF algorithm with the EKF and showed that both algorithms offer similar performance when only the loop filter is replaced, with the KF being optimal due to its lower complexity [86].

Kwang-Hoon Kim and Yao. further optimized the KF algorithm by proposing the Adaptive Kalman Filter (AKF), which improves tracking performance by exploiting the adaptive adjustment capability of the AKF [87,88]. Following this, Cheng combined the Carrier Noise Ratio (CNR) estimation algorithm with AKF. By using the estimated CNR to adjust the KF algorithm, this method further enhances tracking performance [89]. Finally, wang adapted the AKF algorithm to dynamically changing environmental conditions by incorporating factors such as platform dynamics, vibration-induced oscillator noise, and tropospheric phase scintillation, thus achieving stronger tracking performance [90].

The second approach, shown in the right panel of Figure 4, estimates signal parameter errors by using the baseband I and Q values as measurements for the KF algorithm. This approach benefits from the fact that the noise characteristics of the I and Q values nearly satisfy the White Gaussian assumption, which is a key assumption in the KF algorithm. The state equation for this method is [24]:

$$\begin{aligned} \begin{bmatrix} x_{p,k+1} \\ x_{w,k+1} \\ x_{a,k+1} \\ x_{j,k+1} \end{bmatrix} &= \begin{bmatrix} 1 & \Delta T_k & \frac{\Delta T_k^2}{2} & \frac{\Delta T_k^3}{6} \\ 0 & 1 & \Delta T_k & \frac{\Delta T_k^2}{2} \\ 0 & 0 & 1 & \Delta T_k \\ 0 & 0 & 0 & 1 \end{bmatrix} \begin{bmatrix} x_{p,k} \\ x_{w,k} \\ x_{a,k} \\ x_{j,k} \end{bmatrix} \\ &\quad - \begin{bmatrix} \Delta T_k \\ 0 \\ 0 \\ 0 \end{bmatrix} w_{NCO_k} + \mathbf{w}_{\phi k} \\ &= \Phi \mathbf{x}_k - \begin{bmatrix} \Delta T_k \\ 0 \\ 0 \\ 0 \end{bmatrix} w_{NCO_k} + \mathbf{w}_{\phi k} \end{aligned} \tag{13}$$

where x_p is the phase difference between the satellite signal carrier and the local carrier in the GNSS receiver, x_w is the frequency Doppler shift of the satellite signal carrier, x_a is the first-order rate of change of the carrier Doppler shift, and x_j is the second-order rate of change of the carrier Doppler shift. w_{NCO_k} is the angular frequency Doppler shift of the carrier NCO in the GNSS receiver, and Φ is the state transition matrix.

The noise vector $W_n = \begin{bmatrix} W_p & W_w & W_a & W_j \end{bmatrix}^T$ is modeled as discrete Gaussian white noise with a mean of 0 and covariance matrix Q_k [24].

$$\mathbf{Q}_\phi = \begin{bmatrix} Q_p & 0 & 0 & 0 \\ 0 & Q_w & 0 & 0 \\ 0 & 0 & Q_a & 0 \\ 0 & 0 & 0 & Q_j \end{bmatrix} \tag{14}$$

where Q_p is caused by the receiver clock phase bias, Q_w is due to the receiver clock frequency drift, Q_a is caused by acceleration along the LOS, and Q_j is caused by receiver jitter along the line between the satellite and the receiver [24].

$$\mathbf{Q}_{k+1} = \int_0^{\Delta T_k} \mathbf{\Phi}\mathbf{Q}_\phi\mathbf{\Phi}^T\, dt = Q_j \begin{bmatrix} \frac{\Delta T_k^7}{252} & \frac{\Delta T_k^6}{72} & \frac{\Delta T_k^5}{30} & \frac{\Delta T_k^4}{24} \\ \frac{\Delta T_k^6}{72} & \frac{\Delta T_k^5}{20} & \frac{\Delta T_k^4}{8} & \frac{\Delta T_k^3}{6} \\ \frac{\Delta T_k^5}{30} & \frac{\Delta T_k^4}{8} & \frac{\Delta T_k^3}{3} & \frac{\Delta T_k^2}{2} \\ \frac{\Delta T_k^4}{24} & \frac{\Delta T_k^3}{6} & \frac{\Delta T_k^2}{2} & \Delta T_k \end{bmatrix} \tag{15}$$

The measurement equation is [24]:

$$\begin{bmatrix} I_{k+1} \\ Q_{k+1} \end{bmatrix} = \begin{bmatrix} \cos(\Delta\phi_k)R(\Delta\tau_k) \\ \sin(\Delta\phi_k)R(\Delta\tau_k) \end{bmatrix} + \begin{bmatrix} n_k^I \\ n_k^Q \end{bmatrix} \tag{16}$$

Nesreen I. Ziedan was the first to propose the use of the Extended Kalman Filter (EKF) to directly process the I and Q correlation values, resulting in a tracking loop with enhanced dynamic stress resistance and improved sensitivity under weak signal conditions [10]. Building on this foundational work, Xinhua Tang evaluated the performance of EKF-based tracking loops and investigated methods for updating the Numerically Controlled Oscillator (NCO) frequency and phase. His design, which incorporated a four-state control input, significantly improved tracking robustness [91]. Qiliang Chen further advanced the approach by introducing a multidimensional NCO update scheme, leading to superior tracking performance in complex environments [41].

In addition to these efforts, Sun et al. conducted a theoretical comparison between traditional Phase-Locked Loop (PLL)-based structures and Kalman filter-based tracking algorithms, demonstrating that Kalman filters offer lower dynamic stress error and improved steady-state behavior [24]. To address the challenges of weak signal reception, Qin et al. proposed a novel adaptive EKF framework that dynamically updates measurement noise statistics based on innovation sequences, thereby enhancing loop stability and adaptability [92]. Zeng et al. developed an EKF architecture capable of real-time estimation of carrier phase, Doppler shift, Doppler rate, and code phase under high-dynamic conditions, achieving reliable performance at acceleration levels up to 100g [93].

Psiaki and Jung introduced an EKF-based tracking algorithm specifically designed for weak GPS signals, combining code and carrier tracking in a unified estimation framework. Their implementation was shown to maintain lock with signal strengths as low as 15 dB-Hz, making it suitable for high-altitude and scintillation-prone environments [94,95]. Tang et al. emphasized the practical aspects of implementing EKF-based tracking in software-defined receivers and highlighted the importance of appropriate NCO update strategies for achieving high-accuracy PVT (position/velocity/time) solutions [91]. Furthermore, Zhu et al. proposed an EKF-based Vector Delay Lock Loop (VDLL) that leverages cross-satellite coupling to maintain lock even when individual channels momentarily lose tracking, providing an effective solution for robust multi-satellite navigation [96].

Despite the theoretical advantages of Kalman Filter structures, their practical performance remains highly dependent on the accuracy of system models and the characterization of noise statistics. In real-time GNSS tracking scenarios, these conditions are often difficult to satisfy due to the complexity of signal environments. As such, continued research into robust and adaptive filtering techniques, as well as improved state modeling under dynamic and uncertain conditions, is essential to further enhance GNSS receiver performance.

Table 4 provides a structured comparison of the main loop filter optimization techniques used in GNSS tracking systems. It highlights each method's strengths and drawbacks, helping to contextualize their applicability across different scenarios.

Table 4. Summary of loop filter optimization techniques in GNSS tracking.

Filter Type	Advantages	Challenges	Representative References
Wiener Filter	Effective at suppressing thermal and oscillator noise; low implementation complexity.	Fixed gain; less adaptive to environmental changes.	Curran, J. T. (2012) [23]
Kalman Filter	Provides optimal tracking performance with white Gaussian noise; flexible model design.	Sensitive to model inaccuracies; assumes known noise statistics.	Henkel, P. (2009) [33], Lashley, M. (2009) [31], Peng, S. (2012) [35], Liu, W. (2025) [86]
Extended Kalman Filter	Can handle nonlinear measurement equations; effective in dynamic or weak signal scenarios.	Requires Jacobian calculation; highly sensitive to incorrect linearization or modeling.	Ziedan, N. I. (2004) [10], Chen, Q. (2018) [41], Sun, X. (2013) [24], Psiaki, M. L. (2002) [94], Zhu, Z. (2010) [96]

2.3. Vector Tracking Loops

The core principle of VT lies in the fact that the pseudo-range and pseudo-range rates observed by the user are influenced not only by the user's position and velocity but also by the geometry of the satellite constellation. The inherent relationships between the multiple tracking channels of the receiver can be leveraged to enhance tracking performance. The key to the VT algorithm is to fully exploit this inter-channel information and share it across the channels. A flowchart illustrating this process is shown in Figure 5.

Unlike scalar tracking, which utilizes separate loop filters for each channel, VT eliminates these filters and employs a unified navigation filter that links all channels together [30].

The VT algorithm uses the receiver's position, velocity, acceleration, clock bias, clock drift, and other parameters as state variables. To reduce computational complexity, the EKF estimates the errors of these state variables rather than the variables themselves, and adjusts the navigation output based on the estimated state errors.

The state transition equation for VT is [97]:

$$X_{\mathrm{e}} = \begin{bmatrix} \delta x & \delta y & \delta z & \delta \dot{x} & \delta \dot{y} & \delta \dot{z} & \delta \ddot{x} & \delta \ddot{y} & \delta \ddot{z} & b & \dot{b} \end{bmatrix}^T \tag{17}$$

The first nine terms represent the errors in the receiver's position, velocity, and acceleration in the ECEF coordinate system, while the last two terms represent the receiver's clock bias and clock drift errors.

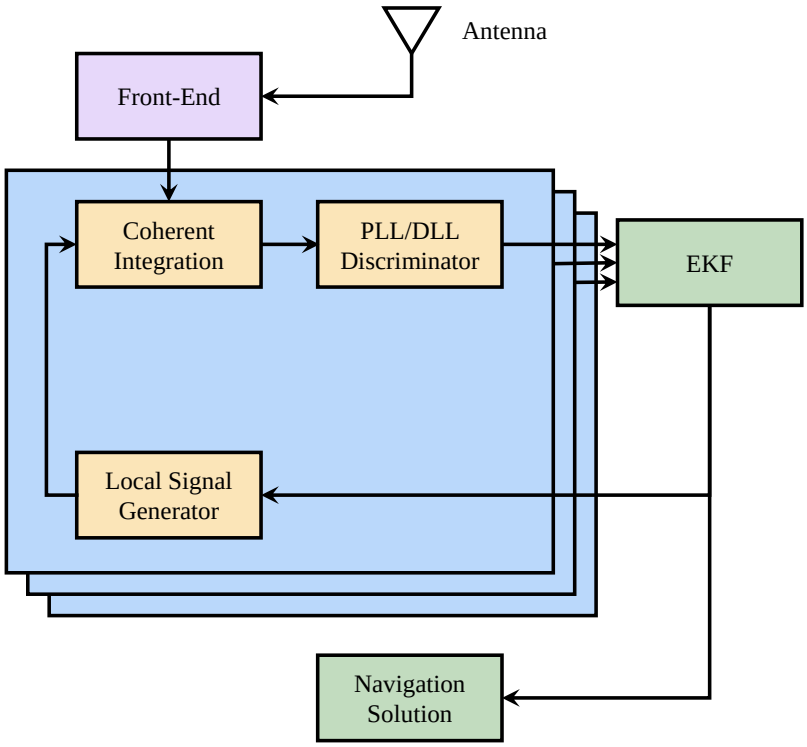


Figure 5. Methods of the vector tracking process.

In practical applications, the state vector can be adapted based on the receiver's dynamic requirements. In low-dynamic scenarios, the effects of the receiver's acceleration and higher-order terms can be neglected to simplify the state vector and filter design. Based on Newton's law of kinematics, the system's state transition equation is:

$$
\begin{aligned}
X_{k+1} &= \begin{bmatrix} \partial x_{k+1} & \partial y_{k+1} & \partial z_{k+1} & \partial \dot{x}_{k+1} & \partial \dot{y}_{k+1} & \partial \dot{z}_{k+1} & \partial \tilde{x}_{k+1} & \partial \tilde{y}_{k+1} & \partial \tilde{z}_{k+1} & b_{k+1} & \dot{b}_{k+1} \end{bmatrix}^T \\
&= \begin{bmatrix} I_{3\times3} & TI_{3\times3} & \frac{T^2}{2}I_{3\times3} & 0 & 0 \\ 0_{3\times3} & I_{3\times3} & TI_{3\times3} & 0 & 0 \\ 0_{3\times3} & 0_{3\times3} & I_{3\times3} & 0 & 0 \\ 0_{3\times1} & 0_{3\times1} & 0_{3\times1} & 1 & T \\ 0_{3\times1} & 0_{3\times1} & 0_{3\times1} & 0 & 1 \end{bmatrix}_{1\times11} \\
&\times \begin{bmatrix} \delta x_k \\ \delta y_k \\ \delta z_k \\ \delta \dot{x}_k \\ \delta \dot{y}_k \\ \delta \dot{z}_k \\ \delta \ddot{x}_k \\ \delta \ddot{y}_k \\ \delta \ddot{z}_k \\ b_k \\ \dot{b}_k \end{bmatrix} + \mathbf{W}_k
\end{aligned}
\tag{18}
$$

This simplifies to:

$$X_{k+1} = FX_k + W_k \tag{19}$$

where T is the KF update time, and W_k is the process noise with mean 0 and covariance Q.

In VT, the EKF takes the pseudo-range residual $\delta\rho$ and the pseudo-range rate residual $\dot{\delta}_\rho$ as the observation quantities. The relationship between the linearized pseudo-range and pseudo-range rate residuals and the state variables is expressed as:

$$\begin{aligned}\mathbf{Z}_k &= \begin{bmatrix} \delta\rho_1 & \cdots & \delta\rho_i & \delta\dot{\rho}_1 & \cdots & \delta\dot{\rho}_i \end{bmatrix}^T \\ &= \begin{bmatrix} -a_{x,1} & -a_{y,1} & -a_{z,1} & 0_{1\times3} & 0_{1\times3} & 1 & 0 \\ -a_{x,i} & -a_{y,i} & -a_{z,i} & 0_{1\times3} & 0_{1\times3} & 1 & 0 \\ 0_{1\times3} & a_{x,1} & a_{y,1} & a_{z,1} & 0_{1\times3} & 0 & -1 \\ \vdots & \vdots & \vdots & \vdots & \vdots & \vdots & \vdots \\ 0_{1\times3} & a_{x,i} & a_{y,i} & a_{z,i} & 0_{1\times3} & 0 & -1 \end{bmatrix} \mathbf{X}_{e,k} + \begin{bmatrix} \eta_1 & \cdots & \eta_i & \xi_1 & \cdots & \xi_i \end{bmatrix}^T \\ &= \mathbf{H}\mathbf{X}_{e,k} + \mathbf{V}_k \end{aligned} \tag{20}$$

where $\mathbf{V}_k$ is the noise term with a mean of 0 and covariance R.

In VT, internal tracking improvements are similar to those in scalar tracking and can be categorized into four approaches: extending coherent integration time, improving discriminator estimation accuracy, enhancing the navigation filter, and hybrid vector/scalar tracking. Since the methods for extending coherent integration time and improving discriminator accuracy are applicable to both scalar and vector loops and have been well discussed in scalar tracking, they will not be revisited here. This section focuses on the evolution of VT, recent advancements in filter optimization, hybrid tracking strategies, and combined applications with IMUs.

2.3.1. Evolution of Vector Tracking Technique

The concept of VT was first proposed by Copps et al. [28]. Later, Spilker introduced the idea of the vector delay-locked loop (VDLL) [98]. Pany [20] then further expanded on tight and deep combination VT structures, which are shown in Figure 6. The primary distinction between tight and deep combinations lies in their relationship with the tracking loop. The tight combination enhances the performance of the tracking loop by integrating auxiliary data, while the deep combination completely replaces the traditional tracking loop, using the navigation solution directly to control signal processing. The deep combination offers greater stability and sensitivity, especially in challenging signal conditions, as it predicts signal parameters based on the navigation solution, reducing reliance on real-time signal tracking.

Lashley et al. [31] demonstrated the advantages of VT in highly sensitive, highly dynamic environments through mathematical derivations and theoretical analysis. Bhattach [99] developed discrete parameter models and transfer function models for VT, including VDLL and vector frequency lock loop (VFLL). Lin [100] categorized the tight combination approach, which integrates the pseudo-range/velocity/time (PVT) solution with signal tracking, as a cascaded VT structure, while the deep combination approach was classified as a centralized VT structure.

Lashley's research on centralized VT algorithms led to several important findings. He implemented the VDLL algorithm using a standalone EKF and showed through simulations that VDLL could rapidly recover signals after masking. Lashley also investigated the VFLL algorithm and concluded that a VT-based receiver could provide continuous location services, even in dense forests [29]. He further demonstrated the thermal noise performance of VDLL and VFLL using Monte Carlo methods and established their empirical tracking thresholds [30]. Additionally, he compared the observational models of VDLL and the standard delay-locked loop (SDLL), noting that VDLL performance depends on the number and geometric distribution of visible satellites [101,102].

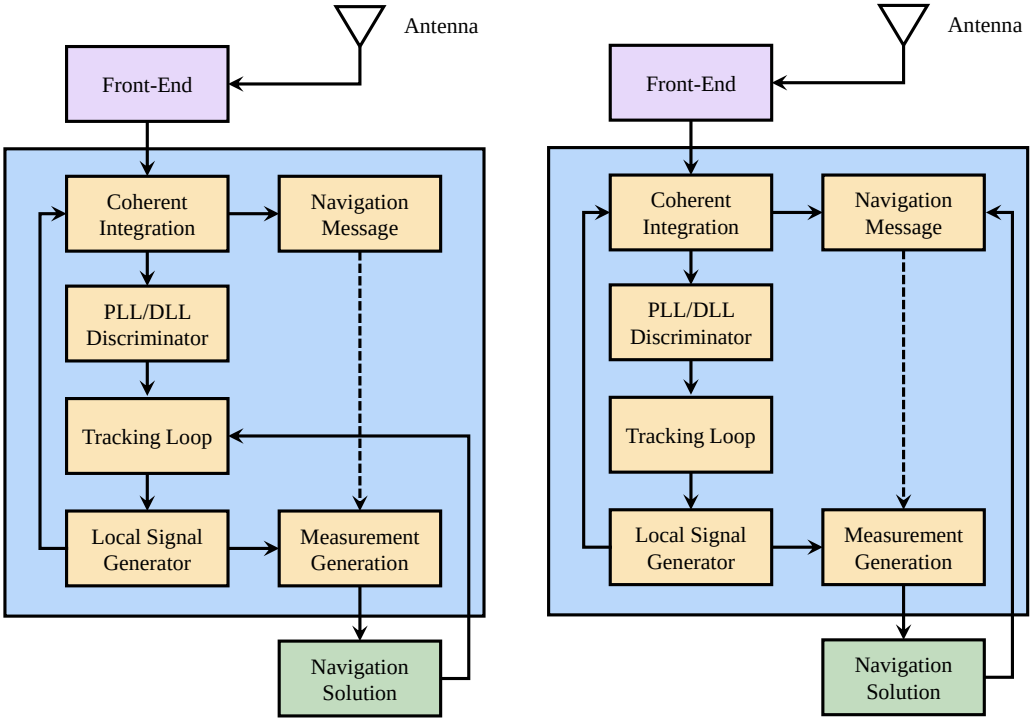


Figure 6. Tight and deep combination methods for vector tracking.

Building on Lashley's work, Yuting Ng proposed a deeply coupled multi-receiver vector tracking (MRVT) architecture to enhance the reliability and robustness of GPS signal tracking and position estimation. MRVT addresses GPS signal intermittency by jointly tracking signals from multiple GPS receivers, thereby improving positioning reliability during weak or intermittent signal conditions.

Several key studies have examined cascaded VT structures. Lin proposed an unweighted cascaded VT structure in which local filters are retained in each channel. This structure degenerates into a scalar tracking system when the locally replicated signals are controlled solely by local filters and into a VT system when controlled exclusively by the PVT solver filters. The local filter serves two main functions: (1) filtering high-frequency signal processing results (such as the output of the signal discriminator) and feeding them into the PVT decoder filter at a lower rate, thus completing the VT algorithm and reducing computational load, and (2) performing signal environment detection. The local filter can identify when the signal environment is unsuitable for VT, at which point local signal generation is directly controlled. Simulation results show that this tracking structure outperforms traditional cascaded VT in terms of environment adaptability [103].

Although much of the research so far has focused on the VT of the carrier frequency or pseudo-code phase, recent developments have shifted toward carrier phase tracking due to increasing demands for higher-accuracy positioning [19,33,39,104]. Pseudo-code positioning typically provides accuracy on the order of meters, while carrier phase positioning achieves accuracies of about 19 cm. The first vector-based carrier phase tracking technique was Co-OP tracking, proposed by Zhodzishky [19]. Co-OP tracking combines a low-bandwidth scalar tracking loop with feedback from a navigation processor and uses a carrier phase discriminator (rather than a carrier frequency discriminator) to calibrate the navigation solution.

Subsequently, the vector carrier phase-locked loop (VPLL) was further developed by Patrick Henkel, José Marc al, and others [33,39,104]. The evolution of VT technology has not only improved GNSS receiver performance in various environments but also laid a solid foundation for future high-precision positioning applications. As research continues, VT

technology is expected to play an increasingly important role in future GNSS applications, especially in the area of carrier phase tracking.

2.3.2. Optimizing the Navigation Filter

In the field of VT, much of the innovation in filter design has focused on enhancing navigation filters within centralized VT architectures. Researchers such as Liu Jing, Patrick Henkel, and Matthew Lashley established the EKF as the mathematical foundation for navigation filters. They derived the principles of EKF mathematically and demonstrated its superior performance [31,33,105], providing a solid theoretical foundation for further advancements in navigation filters.

To address stability issues in VT, Lin Honglei introduced a robust vector tracking loop (RVTL) based on a diagonal weighting matrix. This method effectively resolved stability problems by replacing the traditional weighting matrix [40]. Peng S further enhanced the EKF algorithm by integrating an adaptive covariance matrix, which improved tracking performance [35].

To mitigate the truncation errors introduced by EKF in nonlinear systems, Xiyuan Chen proposed the Iterative EKF (IEKF). This approach reduces bias and estimation errors through iterative operations. By combining it with the Adaptive EKF (AEKF), the Adaptive Iterative EKF (AIEKF) was introduced, resulting in significant improvements in tracking performance [34]. Haotian Yang achieved adaptive EKF VT by adjusting the measurement noise covariance matrix and process noise covariance matrix based on the signal's C/N0 ratio and the innovation sequence [36]. M.A. Farhad further refined the system by fine-tuning all adjustable parameters using a fuzzy method, achieving more accurate adaptive VT [37].

Alternatively, Wei Liu employed the Unscented Kalman Filter (UKF) to replace the EKF, improving positioning accuracy by using pseudo-range and pseudo-range rate errors as measurement parameters [38]. Ning Gao developed a square-root UKF (SRUKF) tracking loop that integrates square-root filtering with an adaptive mechanism. This mechanism dynamically adjusts filter parameters based on signal noise and Doppler feedback errors [38].

In addition, some researchers have explored combining Graph Optimization (GO) techniques with VT to optimize navigation solution estimation. This approach incorporates NLOS-induced distortions into the state vectors for real-time estimation. Compared to the KF-VT approach, the GO-VT framework is more flexible in handling state vector variations, using state transformations and measurement models as constraints to optimize the estimates [106,107].

Currently, most innovations in navigation filters are focused on the EKF algorithm. While several optimization strategies have been proposed, challenges remain in tracking in complex environments. Therefore, further research is needed to optimize navigation filters for improved performance in such environments.

Table 5 summarizes the major optimization techniques for navigation filters in vector tracking systems, highlighting their benefits, limitations, and representative studies.

2.3.3. Vector–Scalar Hybrid Tracking

Senlin Peng [35] was the first to propose leveraging the strengths of both vector and scalar tracking, as shown in Figure 7. In this approach, both the scalar tracking loop (STL) and vector tracking loop (VTL) are implemented. The results from the VTL are used to assist the STL by correcting errors when detected. Building on this concept, José Marçal [39,104] enhanced this hybrid approach through weighted tracking, which resulted in smoother satellite signal processing, improving both efficiency and accuracy.

Table 5. Summary of navigation filter optimization techniques in vector tracking.

Technique	Advantages	Challenges	Representative References
Extended Kalman Filter	Provides baseline for navigation filter; handles non-linearities in measurements.	Sensitive to model errors; requires linearization at each step.	Liu, J. (2011) [105], Henkel, P. (2009) [33], Lashley, M. (2009) [31], Lin, H. (2017) [40]
Adaptive EKF	Dynamically adjusts noise covariance; improves adaptability to signal variation.	Increased computational complexity; tuning difficulties.	Peng, S. (2012) [35], Yang, H. (2021) [36], Farhad, M. (2021) [37], Chen, Q. (2014) [34]
Unscented Kalman Filter	No need for Jacobian; better performance in highly non-linear systems.	Higher complexity; increased memory and computation load.	Liu, W. (2022) [38]
Graph Optimization	Flexible modeling of dynamic state changes and NLOS effects; scalable to large networks.	Model design is complex; sensitive to constraint inconsistencies.	Jiang, C. (2020) [106], Jiang, C. (2022) [107]

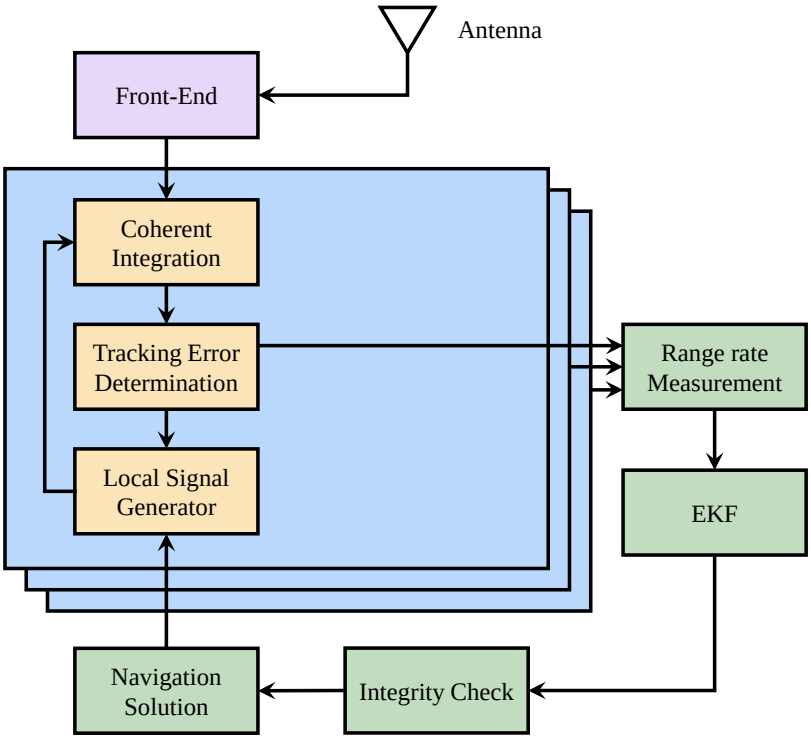


Figure 7. Hybrid vector–scalar tracking loop methods.

Minghui Mou [14] introduced a method using FLL-assisted VPLL, where the carrier loop generates the carrier frequency via the FLL-assisted PLL method based on the KF, maintaining a locked carrier signal. Xinran Zhang and Wei Liu [108,109] later completed the theoretical framework for FLL-assisted VPLL tracking, further demonstrating the advantages of this approach.

Lin Honglei [110] proposed the DU-HTL (Dual Update-Rate Hybrid Tracking Loop), integrating the Dual Update-Rate Kalman Filter (DUKF) and the VFLL. Changhui Jiang [111] combined the PDR (pseudo-range) algorithm with VT to enhance positioning accuracy, broadening the application range of VT technology. Di Liu [112] brought innovation to navigation filters by applying Long Short-Term Memory Recurrent Neural Networks (LSTM-RNNs) to assist KF-based VT, leading to more robust tracking performance.

While several effective hybrid algorithms have been proposed, these methods primarily combine the advantages of scalar and VT (see Table 6). However, challenges remain when tracking in complex environments. Future research should focus on integrating these hybrid methods with emerging technologies, such as deep learning, to further enhance tracking performance.

Table 6. Summary of hybrid vector–scalar tracking techniques.

Technique	Advantages	Challenges	Representative References
VTL-Assisted STL	Combines robustness of vector tracking with simplicity of scalar tracking.	Complexity in switching logic; balancing performance trade-offs.	Peng, S. (2012) [35], Marcal, J. (2016) [39], Marcal, J. (2016) [104]
FLL-Assisted VPLL	Maintains carrier lock with improved sensitivity under weak signal conditions.	Requires careful integration and tuning of FLL and PLL components.	Mou, M. (2021) [14], Zhang, X. (2022) [108], Liu, W. (2022) [109]
Hybrid Tracking Loop	Reduces computational load while preserving tracking accuracy by dual update rates.	Complexity of coordinating multiple update rates; stability concerns.	Lin, H. (2017) [110]
PDR-Enhanced VT	Enhances positioning robustness by fusing pedestrian dead reckoning (PDR) with VT.	Errors in PDR can propagate into the VT solution.	Jiang, C. (2023) [111]
LSTM-RNN-Aided VT	Utilizes deep learning (LSTM) to assist state estimation, improving robustness in complex environments.	Requires large training data; risk of overfitting and poor generalization.	Liu, D. (2020) [112]

2.3.4. Ultra-Tight Combining

The complementary nature of GNSS and INS is most evident in their positioning principles. When satellite signals are weak, INS can operate independently, while GNSS can correct the error that INS accumulates over time. Based on how the systems are integrated, there are three main forms of combination: loose combination, tight combination, and ultra-tight combination. Both loose and tight combinations primarily use GNSS to assist INS for navigation. However, when satellite signals are unavailable, the error accumulation problem in INS remains. Ultra-tight combination, however, allows the combination filter to provide correction information to the receiver based on the tight combination, enabling deeper integration and significantly improving system robustness [113].

The concept of ultra-tight combining emerged in the 1980s, when the US Department of Defense began using INS measurement data to support GPS loop tracking. Around the same time, Cox discussed the use of INS to assist GPS signal acquisition and tracking [114]. With the advent of VT technology, researchers began exploring ultra-tight combining systems based on both vector and scalar tracking, although there has been some disagreement on the definitions of deep combining versus ultra-tight combining.

Researchers like Gautier et al. at Stanford University define deep combining as methods where INS assists GNSS receivers in tracking loops [115]. On the other hand, Gustafson et al. argue that only methods where INS assists in VT of loops should be called deep combining [116]. While the industry lacks a unified definition, the general consensus is that deep combining and ultra-tight combining are essentially the same. Both terms refer to the use of INS information to assist VT of loops [117]. Further, researchers like Niu Xiaogi's team at Wuhan University suggest that deep combining systems can

be classified into scalar deep combining and vector deep combining, depending on the receiver's tracking loop. They propose that ultra-tight combining is equivalent to vector deep combining, meaning that ultra-tight combining always relies on VTL [118,119].

As shown in Figure 8, this ongoing debate underscores the lack of consensus on the definition of ultra-tight combining. For the remainder of this section, the term "deep combining" will be used exclusively to refer to ultra-tight vector-tracking combining.

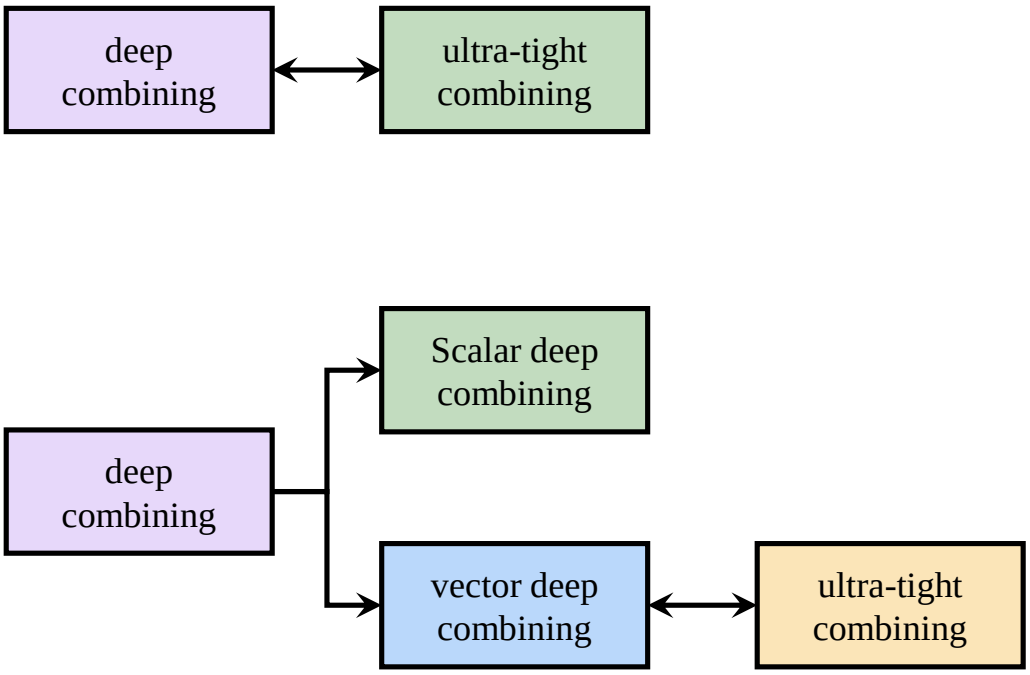


Figure 8. Deep combining methods for INS-assisted vector tracking.

In general, vector-tracking-based ultra-tight integration systems can be classified into centralized ultra-tight integration and cascaded ultra-tight integration, depending on the core structure of the vector-tracking system. Both centralized and cascaded ultra-tight integration directly use the I/Q values from each channel as filter measurements, making them types of coherent ultra-tight integration.

The centralized ultra-tight integration system, first proposed by Spilker [13], uses a single combining filter to process tracking and data fusion information from all channels. This combined output helps correct accumulated INS errors and supports carrier tracking. Ravindra Babu [120] derived key mathematical relationships essential for designing centralized ultra-tight systems. Malek Karaim [121] introduced a novel centralized ultra-tight system by integrating centralized VT with the Reduced Inertial Sensor System (RISS), enhancing GPS receiver robustness and sensitivity in challenging environments. Zhe Yan proposed two ultra-tight coupling approaches based on different observation matrices and introduced an improved deep coupling structure with a multipath error estimator (MPEE), which significantly improves tracking robustness [122–124].

Later, Wei Gao [125] proposed an integrated error modeling scheme for GNSS tracking loops across the entire VT system, derived in an Earth-Centered Fixed-Earth (ECF) framework. This model addresses the error propagation from the combined navigation filter to INS, particularly focusing on acceleration errors caused by the rotation of the LOS direction, a critical factor for dynamic receivers or medium-orbit satellites.

The cascaded ultra-tight integration system, developed by Abbott [126] and others, employs a two-stage filtering approach. The baseband I/Q information is first processed by individual pre-filters in each channel, and the output is passed to the main filter. The pre-filter processes the raw GNSS data, estimates errors in the main filter's code phase and

carrier frequency predictions, and periodically corrects the main filter. The combined filter output then corrects both the INS and adjusts the pseudo-code NCO and carrier NCO by incorporating ephemeris data with the INS output. This system improves the high-dynamic performance of the receiver by measuring velocity and position changes at each update cycle of the VT filters and feeding the data back into the tracking loop [32,127,128].

Dah-Jing Jwo optimized the KF algorithm in cascaded ultra-tight systems using fuzzy logic and the FLAS mechanism, integrating these innovations into the Adaptive Unscented Kalman Filter (AUKF) to develop the FASTUKF algorithm, which maintains excellent estimation accuracy and tracking capability [129,130]. Qunsheng Li [131] and Xi Zhang [132] focused on optimizing conventional pre-filters to reduce errors caused by pseudo-code tracking in cascaded ultra-tight systems. Li [133,134] proposed a GPS/MEMS-SINS ultra-tight integration method using differential carrier phase velocity (TDCP) for loop tracking, reducing carrier loop noise and improving code correlator spacing [86,135]. Baoyu Liu [135] introduced an ultra-tight integration approach that eliminates the tracking loop in the receiver's baseband, relying entirely on INS to track GNSS code signals, employing a moving window-based discontinuous tracking control method for signals of different wavelengths.

In summary, the ultra-tight combination system has become a major area of research in GNSS receiver technology since the 1980s. Continuous innovations in the integration of GNSS and INS have enabled high-performance navigation in diverse environments. However, key technological challenges remain, particularly regarding performance degradation in highly dynamic situations and the use of low-cost MEMS sensors [136].

Table 7 summarizes the two principal approaches to ultra-tight GNSS/INS integration, emphasizing their advantages, challenges, and key references.

Table 7. Summary of ultra-tight combining techniques.

Technique	Advantages	Challenges	Representative References
Centralized Ultra-Tight	Single filter processes multi-channel tracking data; robust against multipath and signal interruptions.	High computational complexity; sensitive to error propagation from model mismatches.	Spilker Jr, J. (1996) [13], Babu, R. (2009) [120], Karaim, M. (2020) [121], Yan, Z. (2021) [122], Yan, Z. (2022) [123], Yan, Z. (2023) [124], Gao, W. (2024) [125]
Cascaded Ultra-Tight	Two-stage structure reduces processing burden and allows adaptive updates; better dynamic adaptability.	Design of pre-filters is critical; potential risk of accumulated estimation errors.	Abbott, A. S. (2003) [126], Lashley, M. (2010) [32], Petovello, M. (2006) [128], Jwo, D.-J. (2010) [129], Jwo, D.-J. (2013) [130], Luo, Y. (2012) [131], Zhang, X. (2016) [132]

Future research should focus on improving performance in dynamic environments and integrating other sensors to enhance ultra-tight combination systems. Additionally, incorporating neural networks for information fusion will be crucial for addressing issues like error model inaccuracies and KF divergence. These advancements are vital for the continued development and practical application of ultra-tight integration systems [113].

2.4. Conventional Approach

Traditional open-loop tracking does not distinguish between the acquisition and tracking phases, treating them as a single process. This method is akin to batch processing, where a complete view of the signal is constructed by analyzing each data batch. During this process, the input signal is correlated with a replica signal generated based on the code and carrier search space. This correlation operation is batch-based, and parallel computation is

achieved through joint time–frequency domain techniques, such as parallel processing of search space transfer correlation coefficients via Fast Fourier Transform (FFT) [137].

The output of the open-loop tracking framework, as shown in Figure 9, is a three-dimensional signal image of the current data batch, with dimensions including code frequency shift, Doppler shift, and signal energy. Utilizing this principle, the CA-code autocorrelation function is computed in parallel for all possible values of the code shift [15]

$$[R(\tau_n)]_{n=1}^{N_{\text{code}}} = \text{Re}\left\{\text{IFFT}\left(\text{FFT}\left([C(A(t_n))]_{n=1}^{N_{\text{code}}}\right)\right) \cdot \text{FFT}\left([C(A(t_n))]_{n=1}^{N_{\text{code}}}\right)\right\} \quad (21)$$

where Re is the real part, $\tau_n = \frac{T_{\text{code}}}{N_{\text{code}}}$ is the CA code period (1 ms), and N_{code} is the number of code samples within the period boundaries. Equation (21) is used to compute in-phase and quadrature correlation values (i and q, respectively) over a 1 ms interval for all possible code shifts and a specific Doppler frequency within the frequency search space.

$$[I_{n,f_h}]_{n=1}^{N_{\text{code}}} = \text{Re}\left\{\text{IDFT}\left(\text{DFT}\left([S(t_n) \cdot C(t_n)]_{n=1}^{N_{\text{code}}}\right)\right) \cdot \text{DFT}\left([C(A(t_n))]_{n=1}^{N_{\text{code}}}\right)\right\} \quad (22)$$

$$[Q_{n,f_h}]_{n=1}^{N_{\text{code}}} = \text{Im}\left\{\text{IDFT}\left(\text{DFT}\left([S(t_n) \cdot C(t_n)]_{n=1}^{N_{\text{code}}}\right)\right) \cdot \text{DFT}\left([C(A(t_n))]_{n=1}^{N_{\text{code}}}\right)\right\} \quad (23)$$

where Re and Im represent the real and imaginary parts, and $C(t_n) = \sin(2\pi(f_{IF} + f_e)t_n) + j\cos(2\pi(f_{IF} + f_e)t_n)$ is the complex carrier. The i and q values are computed for all discrete frequencies of the search space, yielding i_n and q_n, where $n = 1, \ldots, N_{\text{code}}$ and $k = -K, \ldots, K$, thus utilizing the above expression to construct a three-dimensional view, providing the Doppler frequency and pseudo-code phase.

Although traditional open-loop tracking has received less research attention, current innovation trends focus on improvements in discriminators and bridging the gap between open-loop and closed-loop tracking.

2.4.1. Improving Discriminator Estimation Precision

The open-loop tracking method was first proposed by Frank van Graas [42], who discussed the advantages and disadvantages of open-loop and closed-loop tracking in detail. He emphasized how open-loop tracking can utilize FFT to generate a three-dimensional image of the current signal stack, allowing for satellite signal tracking by identifying its maximum value. Esther Anyaegbu further proposed a zoomed FFT technique to reduce the computational complexity of FFT. She evaluated open-loop tracking performance by adjusting the scaling window size and cyclic update rates [43].

Building on this, Kunlun Yan reduced the computational burden of FFT by suggesting it be applied to process I/Q coherent integration results rather than intermediate frequency (IF) data. He proposed that all channels could share a single FFT module and perform a complex squaring operation to mitigate the effect of data bit values. Additionally, a performance comparison between FFT and SFFT (Scaled FFT) was conducted [11].

The study of discriminators has advanced beyond just FFT to explore more accurate estimation methods. For instance, Muhammad Tahir proposed improvements to Kay's method beyond FFT-based discriminators, offering two enhancements to improve performance in low-SNR scenarios [44].

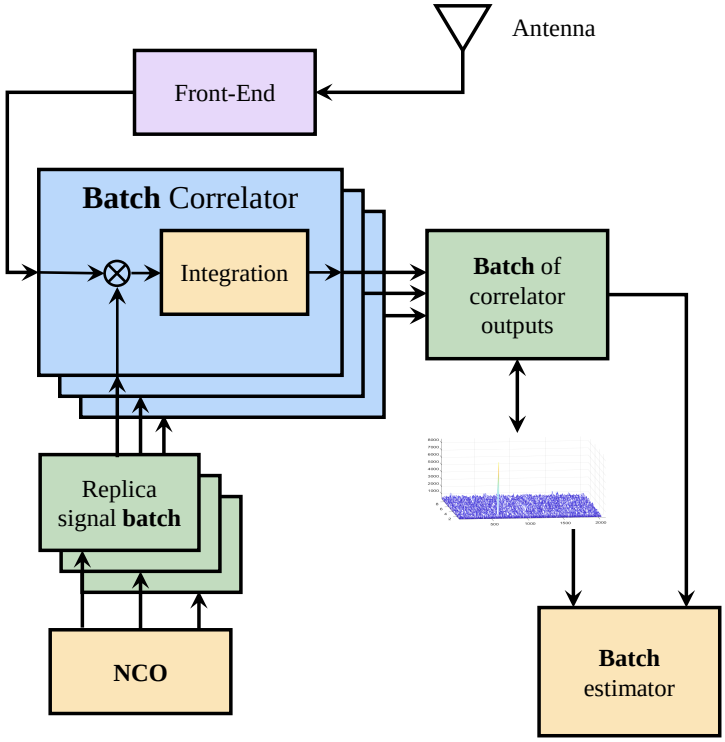


Figure 9. Three-dimensional signal image of the traditional open-loop tracking method.

Additionally, Wang Wen-jing used the UKF for open-loop carrier tracking, with the structure shown in Figure 10. He designed a four-dimensional UKF phase estimator with the state vector $\begin{bmatrix} \hat{\theta}_k & \hat{w}_{d,k} & \hat{w}^1_{d,k} & \hat{w}^2_{d,k} \end{bmatrix}$, where $\hat{\theta}_k$ represents the carrier phase, $\hat{w}_{d,k}$ is the Doppler shift, and $\hat{w}^1_{d,k}$ and $\hat{w}^2_{d,k}$ are the first- and second-order Doppler shift change rates. Shuai Han introduced a compensator after the UKF estimator to adaptively adjust the estimated four-dimensional state vectors [138].

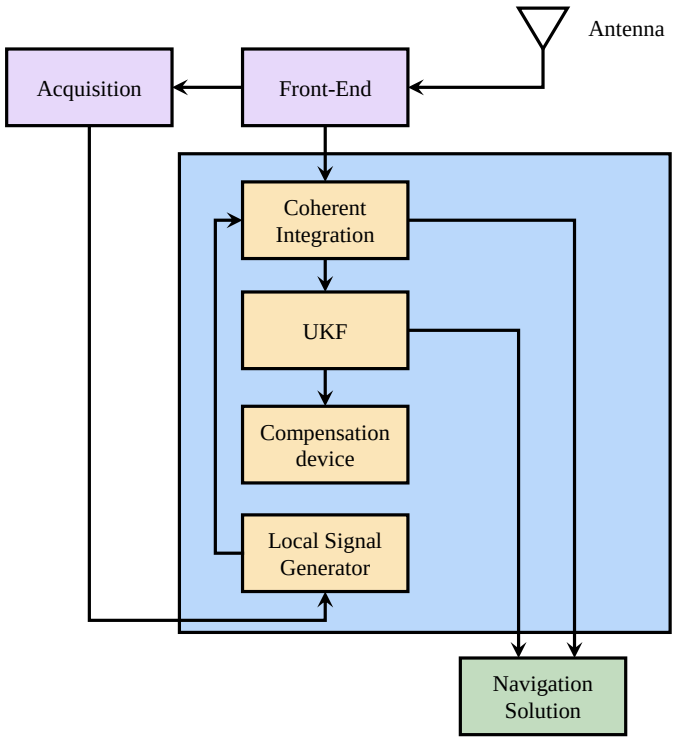


Figure 10. Methods of a four-dimensional unscented KF for open-loop carrier tracking.

Tian Jin proposed an open-loop tracking algorithm based on the dual Kalman Filter (DKF), which uses carrier frequency and pseudo-code phase differences from different channels as observation vectors and the receiver's position and velocity as state vectors. This approach improves tracking accuracy [45]. Chao Wu proposed a two-stage frequency estimation method combining coarse frequency estimation using discrete Fourier transform (DFT) and fine frequency estimation based on ML estimation (MLE) [46].

As open-loop tracking discriminators have evolved, various solutions have emerged. Initially, FFT was applied directly to IF data processing, which later evolved into basic coherent integral signal processing. These advances have gradually alleviated the high computational requirements of traditional open-loop tracking. Future research should focus on further improving the accuracy of discriminators based on coherent integral signal processing.

Table 8 provides a summary of the major discriminator optimization techniques developed for open-loop tracking, highlighting their respective advantages, challenges, and representative references.

Table 8. Summary of discriminator optimization techniques for open-loop tracking.

Technique	Advantages	Challenges	Representative References
FFT Discriminator	Generates 3D signal image for robust satellite signal detection.	High computational complexity; limited real-time applicability.	Van Graas, F. (2005) [42], Anyaegbu, E. (2006) [43], Yan, K. (2016) [11]
Enhanced Kay's Method	Improved estimation accuracy in low SNR scenarios.	Increased algorithm complexity; sensitive to model mismatch.	Tahir, M. (2012) [44]
Four-Dimensional UKF Estimator	Captures high-order Doppler effects; robust against dynamics.	Increased state dimension leads to higher computational load.	Han, S. (2010) [138], Jin, T. (2020) [45]
Two-Stage Frequency Estimation	Combines coarse and fine estimation for improved frequency accuracy.	Requires careful transition design between coarse and fine stages.	Wu, C. (2022) [46]

2.4.2. Open-Loop and Closed-Loop Hybrid Tracking

The concept of hybrid open-loop and closed-loop tracking was first introduced by Georges Stienne, who explored open-loop phase tracking supported by closed-loop pseudocode tracking, as shown in Figure 11. He chose a KF with a likelihood-maxima fusion operator based on the von Mises distribution as the estimator [47]. Stienne extended the estimation dimension of the estimator and optimized open-loop tracking by introducing a detector in the closed-loop pseudocode tracking loop to identify and correct pseudo-code phase errors [48].

Muhammad Tahir addressed the limitations of conventional closed-loop tracking, which lacks degrees of freedom, by proposing a quasi-open-loop tracking structure that combines both open-loop and closed-loop methods. This structure simplifies filter design by updating parameters at three different rates, thus increasing the degrees of freedom within the system [49].

Honglei Lin proposed an intermittent tracking method for open-loop GNSS signals using Kalman filtering, thoroughly analyzing the relationship between tracking accuracy and duty cycle [48].

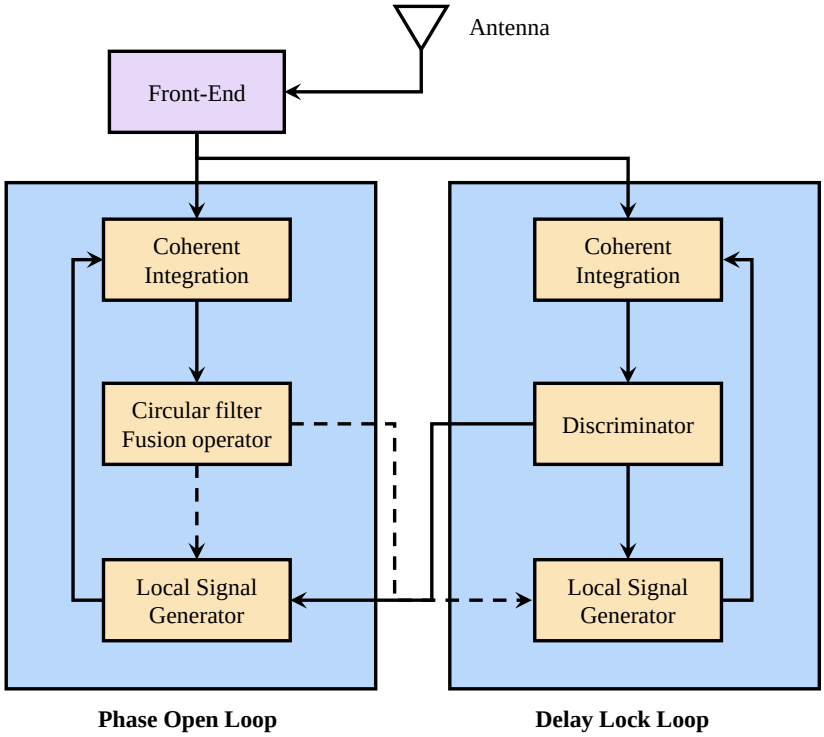


Figure 11. Hybrid open-loop and closed-loop tracking methods.

In summary, the development of hybrid open-loop and closed-loop tracking techniques, which combine the advantages of both approaches, has evolved from initial concept proposals to the realization of various technologies. The introduction and refinement of these techniques not only enhance the robustness of GNSS receivers in complex environments but also provide new solutions for high-precision positioning.

Direct Position Estimation

The concept of DPE, initially proposed by Pau Closas, deviates from the traditional receiver approach that relies on Time Difference of Arrival (TDOA) estimation, instead estimating the position directly from the received data. The block diagram for the DPE flow is shown in Figure 12. This method combines the data from all visible satellites to jointly perform position estimation, overcoming biases caused by multipath effects or transient satellite link blockage. Based on the invariance principle of position estimation, Closas derives the ML estimate for the position from the ML estimate of the synchronization parameters [48].

$$\hat{\chi}_{n+1} = \underset{\chi}{\operatorname{argmax}} \left\{ \sum_{i=1}^{M} \Lambda_i \left(\tau_i(\chi), f_{d_i}(\chi) \right) \right\} = \hat{\chi}_n \tag{24}$$

Here, M represents the number of visible satellites, and $\Lambda_i(\tau_i(\chi), f_{d_i}(\chi))$ represents the correlation value between the local signal of the i-th visible satellite at the selected position χ and the received signal. The magnitude of the correlation value is determined by the code phase and Doppler frequency of the local signal.

The innovation of the DPE method lies in its ability to naturally incorporate prior information, which traditional synchronization-based methods struggle to achieve due to difficulties in modeling the evolution of these parameters. The user's coordinate information can be obtained from motion models, tightly integrated IMU, or other potential sources of user motion data, thus enhancing the sensitivity of satellite signal tracking [48]. Despite the inherently high sensitivity of the DPE algorithm, the main challenge lies in its high implementation complexity. Subsequent research has focused on optimizing the

algorithm, integrating sensor fusion, and combining various filtering methods to improve stability, ease of implementation, and performance in complex environments.

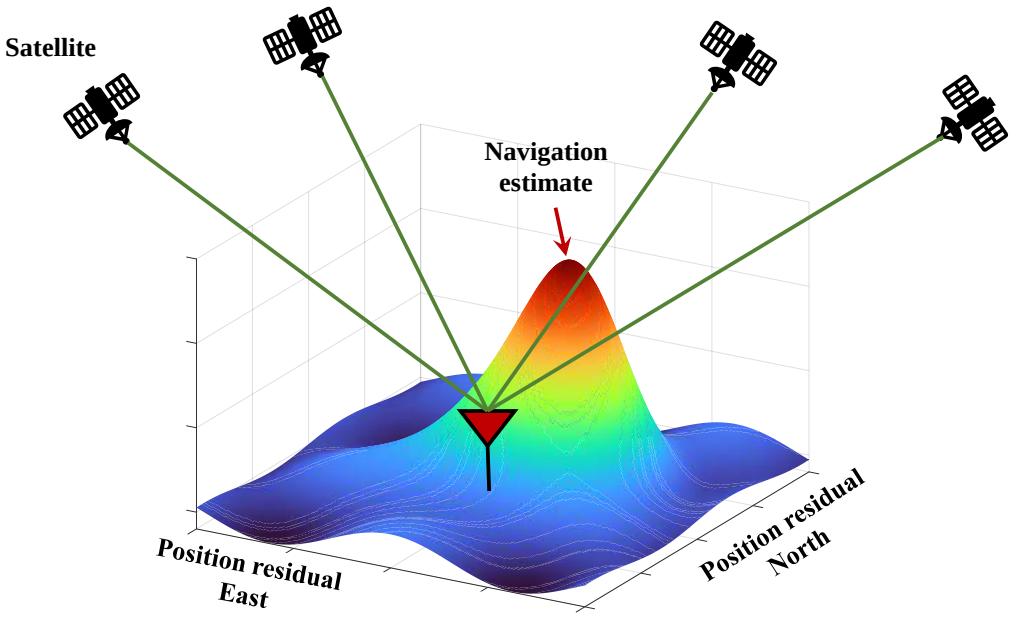


Figure 12. Direct Position Estimation (DPE) method.

Alon Amar et al. [53,54,139] conducted a detailed comparison between the DPE method and traditional synchronization techniques, demonstrating that both approaches exhibit consistent asymptotic unbiasedness and efficient estimation performance. Their study also validated the robustness of DPE under various challenging conditions, including multipath, fading, and dynamic user scenarios. Building on this, Pau Closas derived the Cramer–Rao lower bounds (CRLB) for both conventional and DPE-based positioning methods and provided the corresponding root mean square error (RMSE) performance analysis [51]. Baker et al. [140] evaluated DPE performance in high-dynamic environments, such as scenarios with high-speed motion and rapid acceleration changes, and confirmed that DPE maintains superior positioning accuracy even when GPS signal quality is degraded. In the context of urban canyon environments, Huang et al. [141] investigated DPE's resilience against multipath interference. Their results indicated that, by improving the signal modeling to better account for multipath and Non-Line-of-Sight (NLOS) effects, DPE significantly outperforms conventional receivers in complex urban environments. Vicenzo et al. [142] further validated these findings through field tests in various urban settings, showing that DPE outperforms conventional scalar tracking methods in lightly obstructed environments, although its performance degrades under severe multipath conditions.

In terms of methodological innovation, Closas extended DPE into a Bayesian framework by proposing a Bayesian DPE algorithm, exploring multiple possible state space formulations, and validating the feasibility of the approach through simulations [50]. He also integrated DPE with inertial measurement unit (IMU) data and compared the performance of different fusion filtering approaches [52]. To enhance satellite visibility under complex environments, Jia and Guo [143] proposed a dual-mode DPE receiver design based on GPS L1 and BeiDou B1C signals, thereby improving the robustness of the DPE system by leveraging signals from both systems. In addition, Ng and Gao [144] introduced a method that treats NLOS GPS signals as useful LOS signals, significantly improving DPE positioning accuracy and robustness in urban environments.

Regarding algorithmic optimization, Athindran Ramesh Kumar incorporated modern estimation techniques into DPE by employing the Unscented Kalman Filter (UKF) to

optimize the likelihood estimation process, thereby enhancing overall performance [55]. Yuting Ng proposed a novel initialization strategy, categorizing navigation states into two groups—position and clock offset variations and velocity and clock drift variations—followed by vector-based computation to improve estimation efficiency and accuracy [145].

In the domain of multi-sensor fusion, Yuting Ng further developed an approach that combines DPE-estimated navigation solutions with image-based map matching, closed-loop GPS signal tracking, and camera image tracking. By incorporating known static GPS receiver positions as a priori information, this method simplifies the joint estimation of 3D position, clock bias, 3D velocity, and clock drift parameters, thereby enhancing the robustness of DPE under multipath conditions. Additionally, Ng proposed a technique to convert originally interfering NLOS signals into useful navigation information [56].

Focusing on DPE architecture, Arthur Hsi-Ping Chu [57] proposed the Multi-Receiver DPE (MR-DPE) technique, which forms a network by connecting multiple DPE receivers with known antenna baselines, fuses their signal measurements, constructs a network-wide likelihood function, and solves for the overall Position/Velocity/Time (PVT) solution using maximum-likelihood (ML) estimation. To reduce the computational complexity of DPE algorithms, Ondrej Daniel introduced the Relaxed DPE (RDPE) approach [53], which precomputes correlation functions on discrete grids and neglects temporal correlations between noisy samples, significantly decreasing computational load.

Furthermore, recent research has introduced emerging technologies into DPE. Vicenzo et al. [146] explored the integration of machine learning techniques, such as Random Forest regression, to assist DPE in urban environments heavily affected by multipath and NLOS effects, demonstrating that machine learning can effectively correct DPE positioning errors. Tang, Li, and Closas [147] proposed a single-difference code-based DPE method, which mitigates satellite clock errors and atmospheric delays, resulting in significantly improved positioning accuracy compared to conventional DPE methods.

Table 9 summarizes the major Direct Position Estimation (DPE) techniques developed in recent years, highlighting their advantages and representative studies. Despite these advancements, all DPE approaches inherently suffer from high computational demands.

As the technology continues to evolve, DPE holds significant potential to enhance the accuracy and robustness of satellite navigation. However, there are still relatively few studies on DPE technology, and it faces challenges in entering the consumer market due to its high computational requirements. Nevertheless, as DPE algorithms are optimized, they are expected to bring revolutionary advances to GNSS navigation systems in the future.

Table 9. Summary of Direct Position Estimation (DPE) methods.

Method	Advantages	Representative References
Maximum-Likelihood Estimation (MLE)-Based DPE	Foundational DPE framework; derives ML estimate directly from received signals.	Closas, P. (2007) [48]
Bayesian DPE	Extends DPE to Bayesian framework; enables prior information fusion.	Closas, P. (2008) [50], Closas, P. (2010) [52]
UKF-Enhanced DPE	Applies unscented Kalman Filter to optimize DPE likelihood estimation.	Ramesh Kumar, A. (2015) [55]
Multi-Receiver DPE	Fuses signals from multiple receivers to jointly estimate PVT solution.	Chu, A. H.-P. (2019) [57]

Table 9. *Cont.*

Method	Advantages	Representative References
Relaxed DPE	Reduces computational complexity via precomputed correlation functions.	Closas, P. (2017) [53]
Dual-Mode DPE	Utilizes multi-constellation signals to enhance robustness in challenging environments.	Jia, Q. (2025) [143]
NLOS-Aided DPE	Treats NLOS signals as useful reflections to improve positioning accuracy.	Ng, Y. (2016) [144]
Machine Learning-Assisted DPE	Integrates random forest regression to mitigate multipath/NLOS errors.	Vicenzo, S. (2024) [146]
Single-Difference Code-Based DPE	Reduces satellite clock and atmospheric errors to enhance DPE accuracy.	Tang, S. (2024) [147]

3. Results

This section presents comparative experiments to assess the performance of different tracking techniques under varying sensitivity conditions. The tracking techniques evaluated include Salor Tracking, VT, the Conventional Approach, and DPE. The primary evaluation metrics are positioning error and tracking error.

To simulate varying signal strength environments, the experiments modulated the carrier-to-noise density ratio CNR of the received signals. The CNR range was set from 45 dB-Hz to 24 dB-Hz with a step size of 1 dB. To ensure consistency across different tracking methods, all techniques were configured with identical parameters: a loop bandwidth of 50 Hz and a fixed integration time of 1 ms. The experimental environment was static, with the receiver held stationary to isolate the effects of satellite dynamics, thereby eliminating interference from receiver motion. The signal source employed a multi-satellite simulation with a fixed number of six satellites, broadcasting GPS L1 C/A signals.

The positioning error results are shown in Figure 13. The figure provides a detailed illustration of the positioning error variations in three coordinate directions (X, Y, Z) for Salor Tracking, VT, the Conventional Approach, and DPE. It can be observed from the figure that there are significant differences in the error magnitude and fluctuation among different tracking methods across various coordinate axes. Specifically, Salor Tracking and VT demonstrate superior positioning accuracy compared to the Conventional Approach and DPE, particularly under low-CNR conditions, where their advantage is more pronounced. However, in terms of stability, VT and DPE exhibit better performance with smaller error fluctuations, while Salor Tracking and the Conventional Approach show relatively larger error variations. These results are consistent with the theoretical analysis presented earlier, indicating that vector tracking methods (such as VT and DPE) have certain advantages in terms of accuracy and stability in complex environments.

To further evaluate the sensitivity characteristics of different tracking methods, the tracking error results are presented in Figure 14. It can be clearly observed from the figure that the error of all tracking methods increases gradually with the decrease in the CNR. Under high CNR conditions, Salor Tracking and VT exhibit similar performance with comparable error levels. However, as CNR decreases, VT outperforms Salor Tracking and demonstrates superior stability in low-signal-to-noise-ratio environments. In contrast, the Conventional Approach and DPE show more significant error fluctuations, with error values generally higher than those of Salor Tracking and VT. Nevertheless, the Conventional Approach and DPE exhibit similar stability to VT, maintaining relatively stable error levels.

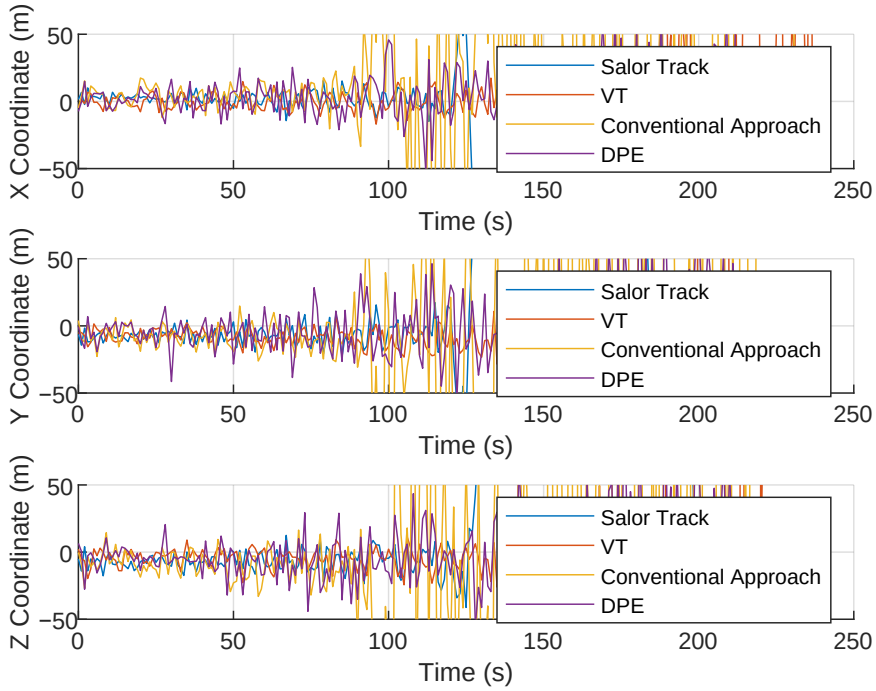


Figure 13. Positioning error vs. C/N_0.

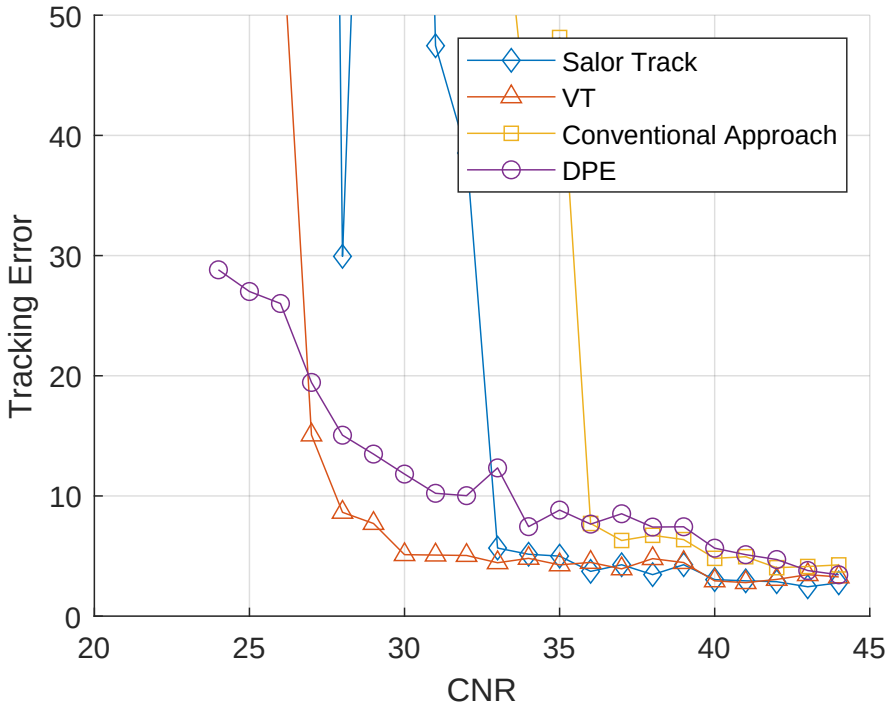


Figure 14. Tracking error standard deviation vs. C/N_0 for different tracking methods.

These results validate the previous analysis: closed-loop tracking methods have higher sensitivity than open-loop tracking methods, and estimation-based methods exhibit higher sensitivity under low-CNR conditions. Overall, in terms of sensitivity metrics, vector tracking outperforms scalar tracking, and closed-loop tracking outperforms open-loop tracking. These findings provide a solid basis for selecting high-sensitivity tracking techniques suitable for complex environments.

4. Conclusions

This paper presents a comprehensive review of the development trajectory of high-sensitivity tracking technologies in GNSS. It systematically analyzes the transition from traditional closed-loop tracking toward open-loop, hybrid, and deeply integrated architectures. Key strategies such as coherent integration time extension, discriminator design, loop filter optimization, vector tracking (VT), and Direct Position Estimation (DPE) are evaluated in terms of their adaptability to weak signal environments. By comparing various approaches across performance and complexity dimensions, this review outlines the current technical trends and challenges in the design of robust GNSS tracking systems.

Despite significant advancements, several critical challenges remain. First, the navigation filters in vector tracking and the loop filters in scalar tracking are highly dependent on accurate system models and noise statistics, limiting their robustness under various environmental conditions [33,58]. Second, the phase noise of consumer-grade oscillators restricts the achievable coherent integration time, posing a major bottleneck for sensitivity improvement [26,60,70]. Third, open-loop tracking has certain advantages in terms of dynamics and sensitivity, and its computational complexity hinders implementation on resource-constrained platforms [48,53,146].

In response to the aforementioned challenges, future research is likely to focus on the following three key directions.

1. Integrating deep learning techniques into filter structures to enhance adaptability and robustness. Deep learning has the capability to model and adaptively adjust signal characteristics under various environmental conditions, thereby achieving more accurate state estimation in complex and dynamic channel environments. By incorporating deep learning algorithms, the parameters of the filters can be dynamically adjusted to maintain optimal performance in challenging scenarios;
2. Current research on collaborative estimation schemes requires strong signals, but complex scenarios are often characterized by weak signals [12]. Therefore, there is a need to continue developing multi-channel collaborative estimation schemes for oscillator noise. By integrating external signal data, such as 4G/5G communication signals, the impact of oscillator noise on the signal can be reduced, coherent integration time can be extended, and the overall system performance can be improved;
3. Design low-complexity approximations for open-loop tracking to better align with hardware resource constraints. By optimizing the algorithm structure and simplifying the computational process, it is possible to reduce the computational complexity of open-loop tracking without significantly compromising sensitivity and dynamic performance, thereby enhancing its feasibility for practical deployment;

Author Contributions: Z.G., H.L. and G.O.: Conceptualization; Writing—Original Draft; Writing—Review and Editing. Z.L. (Zhe Liu), Z.L. (Zengjun Liu), and L.H.: Writing—-Original Draft; Writing—Review and Editing. All authors have read and agreed to the published version of the manuscript.

Funding: This work was supported by the National Natural Science Foundation of China (NSFC) under grant number U20A20193.

Data Availability Statement: The original contributions presented in the study are included in the article, further inquiries can be directed to the corresponding author.

Conflicts of Interest: The authors declare that they have no known competing financial interests or personal relationships that could have appeared to influence the work reported in this paper.

References

1. Hameed, A.; Ahmed, H.A. Survey on indoor positioning applications based on different technologies. In Proceedings of the 2018 12th International Conference on Mathematics, Actuarial Science, Computer Science and Statistics (MACS), Karachi, Pakistan, 24–25 November 2018; IEEE: Piscataway, NJ, USA, 2018; pp. 1–5.
2. Gao, Z.; Shen, W.; Zhang, H.; Niu, X.; Ge, M. Real-time kinematic positioning of INS tightly aided multi-GNSS ionospheric constrained PPP. *Sci. Rep.* **2016**, *6*, 30488. [CrossRef] [PubMed]
3. Canales, J. Navigating the history of GPS. *Nat. Electron.* **2018**, *1*, 610–611. [CrossRef]
4. Rezwan, S.; Choi, W. Artificial intelligence approaches for UAV navigation: Recent advances and future challenges. *IEEE Access* **2022**, *10*, 26320–26339. [CrossRef]
5. Kaplan, E.D.; Hegarty, C. *Understanding GPS/GNSS: Principles and Applications*; Artech House: Norwood, MA, USA, 2017.
6. Ding, X.; Yang, Y.; Chen, J. Improved high-sensitivity partial-matched filter with FFT-based acquisition algorithm for BDS-2 and BDS-3 signals with secondary code modulation. *GPS Solut.* **2023**, *27*, 143. [CrossRef]
7. Kuutti, S.; Fallah, S.; Katsaros, K.; Dianati, M.; Mccullough, F.; Mouzakitis, A. A survey of the state-of-the-art localization techniques and their potentials for autonomous vehicle applications. *IEEE Internet Things J.* **2018**, *5*, 829–846. [CrossRef]
8. Ye, Z.; Zhao, G.; Yang, M.; Chen, P.-Y. Review on wearable antennas: Part 2: Recent advances and applications. *IEEE Antennas Propag. Mag.* **2025**, 2–13. [CrossRef]
9. Ashraf, I.; Hur, S.; Park, Y. Smartphone sensor based indoor positioning: Current status, opportunities, and future challenges. *Electronics* **2020**, *9*, 891. [CrossRef]
10. Ziedan, N.I.; Garrison, J.L. Extended Kalman filter-based tracking of weak GPS signals under high dynamic conditions. In Proceedings of the 17th International Technical Meeting of the Satellite Division of the Institute of Navigation (ION GNSS 2004), Long Beach, CA, USA, 21–24 September 2004; pp. 20–31.
11. Yan, K.; Ziedan, N.I.; Zhang, H.; Guo, W.; Niu, X.; Liu, J. Weak GPS signal tracking using FFT discriminator in open loop receiver. *GPS Solut.* **2016**, *20*, 225–237. [CrossRef]
12. Feng, X.; Zhang, T.; Niu, X.; Pany, T.; Liu, J. Improving GNSS carrier phase tracking using a long coherent integration architecture. *GPS Solut.* **2023**, *27*, 37. [CrossRef]
13. Spilker, J.J., Jr.; Axelrad, P.; Parkinson, B.W.; Enge, P. *Global Positioning System: Theory and Applications, Volume I*; American Institute of Aeronautics and Astronautics: Reston, VA, USA, 1996.
14. Mou, M.; Hu, Y.; Gu, M.; Wang, S.; Liu, W. A vector tracking structure of FLL-assisted PLL for GNSS receiver. In Proceedings of the China Satellite Navigation Conference (CSNC 2021) Proceedings: Volume III, Nanchang, China, 22–25 May 2021; Springer: Berlin/Heidelberg, Germany, 2021; pp. 252–264.
15. Van Graas, F.; Soloviev, A.; de Haag, M.U.; Gunawardena, S. Closed-loop sequential signal processing and open-loop batch processing approaches for GNSS receiver design. *IEEE J. Sel. Top. Signal Process.* **2009**, *3*, 571–586. [CrossRef]
16. Meyr, H. *Digital Communication Receivers: Synchronization, Channel Estimation, and Signal Processing*; Wiley: Hoboken, NJ, USA, 1998.
17. Kazemi, P.L. Optimum digital filters for GNSS tracking loops. In Proceedings of the 21st International Technical Meeting of the Satellite Division of The Institute of Navigation (ION GNSS 2008), Savannah, GA, USA, 16–19 September 2008; pp. 2304–2313.
18. Van Diggelen, F. *A-GPS: Assisted GPS, GNSS, and SBAS*; Artech House: Norwood, MA, USA, 2009.
19. Zhodzishsky, M.; Yudanov, S.; Veitsel, V.; Ashjaee, J. Co-op tracking for carrier phase. In Proceedings of the 11th International Technical Meeting of the Satellite Division of The Institute of Navigation (ION GPS 1998), Nashville, TN, USA, 15–18 September 1998; pp. 653–664.
20. Pany, T.; Kaniuth, R.; Eissfeller, B. Deep integration of navigation solution and signal processing. In Proceedings of the 18th International Technical Meeting of the Satellite Division of The Institute of Navigation (ION GNSS 2005), Fort Worth, TX, USA, 25–28 September 2005; pp. 1095–1102.
21. Lian, P.; Lachapelle, G.; Ma, C. Improving tracking performance of PLL in high dynamics applications. In Proceedings of the 2005 National Technical Meeting of the Institute of Navigation, San Diego, CA, USA, 22–24 January 2005; pp. 1042–1052.
22. Ren, T.; Petovello, M.; Basnayake, C. Requirements analysis for bit synchronization and decoding in a standalone high-sensitivity GNSS receiver. In Proceedings of the 2012 Ubiquitous Positioning, Indoor Navigation, and Location Based Service (UPINLBS), Helsinki, Finland, 3–4 October 2012; IEEE: Piscataway, NJ, USA, 2012; pp. 1–9.
23. Curran, J.T.; Lachapelle, G.; Murphy, C.C. Digital GNSS PLL design conditioned on thermal and oscillator phase noise. *IEEE Trans. Aerosp. Electron. Syst.* **2012**, *48*, 180–196. [CrossRef]
24. Sun, X.; Qin, H.; Niu, J. Comparison and analysis of GNSS signal tracking performance based on Kalman filter and traditional loop. *WSEAS Trans. Signal Process.* **2013**, *9*, 99–107.
25. Guo, W.; Yan, K.; Zhang, H.; Niu, X.; Shi, C. Double stage NCO-based carrier tracking loop in GNSS receivers for city environmental applications. *IEEE Commun. Lett.* **2014**, *18*, 1747–1750. [CrossRef]

26. Chen, S.; Gao, Y.; Lin, T. Effect and mitigation of oscillator vibration-induced phase noise on carrier phase tracking. *GPS Solut.* **2017**, *21*, 1515–1524. [CrossRef]
27. Li, J.; Zhao, L.; Hou, Y.; Hu, Y. A new tracking technique with the memory discriminator for high sensitivity GNSS receivers. In Proceedings of the 2018 IEEE 4th International Conference on Computer and Communications (ICCC), Chengdu, China, 7–10 December 2018; IEEE: Piscataway, NJ, USA, 2018; pp. 959–962.
28. Copps, E.; Geier, G.; Fidler, W.; Grundy, P. Optimal processing of GPS signals. *Navigation* **1980**, *27*, 171–182. [CrossRef]
29. Lashley, M.; Bevly, D.M. Analysis of discriminator based vector tracking algorithms. In Proceedings of the 2007 National Technical Meeting of the Institute of Navigation, San Diego, CA, USA, 22–24 January 2007; pp. 570–576.
30. Lashley, M.; Bevly, D.M. Vector delay/frequency lock loop implementation and analysis. In Proceedings of the 2009 International Technical Meeting of The Institute of Navigation, Anaheim, CA, USA, 22–25 January 2009; pp. 1073–1086.
31. Lashley, M.; Bevly, D.M.; Hung, J.Y. Performance analysis of vector tracking algorithms for weak GPS signals in high dynamics. *IEEE J. Sel. Top. Signal Process.* **2009**, *3*, 661–673. [CrossRef]
32. Lashley, M.; Bevly, D.M.; Hung, J.Y. Analysis of deeply integrated and tightly coupled architectures. In Proceedings of the IEEE/ION Position, Location and Navigation Symposium, Portland, OR, USA, 20–23 April 2020; IEEE: Piscataway, NJ, USA, 2010; pp. 382–396 .
33. Henkel, P.; Giger, K.; Gunther, C. Multifrequency, multisatellite vector phase-locked loop for robust carrier tracking. *IEEE J. Sel. Top. Signal Process.* **2009**, *3*, 674–681. [CrossRef]
34. Chen, X.; Wang, X.; Xu, Y. Performance enhancement for a GPS vector-tracking loop utilizing an adaptive iterated extended Kalman filter. *Sensors* **2014**, *14*, 23630–23649. [CrossRef]
35. Peng, S.; Morton, Y.; Di, R. A multiple-frequency GPS software receiver design based on a vector tracking loop. In Proceedings of the 2012 IEEE/ION Position, Location and Navigation Symposium, Myrtle Beach, SC, USA, 23–26 April 2012; IEEE: Piscataway, NJ, USA, 2012; pp. 495–505.
36. Yang, H.; Zhou, B.; Wang, L.; Wei, Q.; Ji, F.; Zhang, R. Performance and evaluation of GNSS receiver vector tracking loop based on adaptive cascade filter. *Remote Sens.* **2021**, *13*, 1477. [CrossRef]
37. Farhad, M.; Mosavi, M.; Abedi, A. Fully adaptive smart vector tracking of weak GPS signals. *Arab. J. Sci. Eng.* **2021**, *46*, 1383–1393. [CrossRef]
38. Liu, W.; Huang, H.; Hu, Y.; Mou, M.; Hsieh, T.H.; Hu, Q.; Wang, S. Improved GNSS vector tracking loop to enhance the navigation performance of USV. *Ocean Eng.* **2022**, *258*, 111865. [CrossRef]
39. Marcal, J.; Nunes, F.; Sousa, F.M. Performance of a scintillation robust vector tracking for GNSS carrier phase signals. In Proceedings of the 2016 8th ESA Workshop on Satellite Navigation Technologies and European Workshop on GNSS Signals and Signal Processing (NAVITEC), Noordwijk, The Netherlands, 14–16 December 2016; IEEE: Piscataway, NJ, USA, 2016; pp. 1–8.
40. Lin, H.; Huang, Y.; Tang, X.; Sun, G.; Ou, G. A robust vector tracking loop based on diagonal weighting matrix for navigation signal. *Adv. Space Res.* **2017**, *60*, 2607–2619. [CrossRef]
41. Chen, Q.; Wu, X.; Liang, J.; Zeng, C. An EKF-based tracking loop filter algorithm in GNSS receiver for ultra high dynamic environment: The experiment results. In Proceedings of the IECON 2018-44th Annual Conference of the IEEE Industrial Electronics Society, Washington, DC, USA, 2018; pp. 2802–2808.
42. Van Graas, F.; Soloviev, A.; de Haag, M.U.; Gunawardena, S.; Braasch, M. Comparison of two approaches for GNSS receiver algorithms: Batch processing and sequential processing considerations. In Proceedings of the 18th International Technical Meeting of the Satellite Division of The Institute of Navigation (ION GNSS 2005), Fort Worth, TX, USA, 25–28 September 2005; pp. 200–211.
43. Anyaegbu, E. A frequency domain quasi-open loop tracking loop for GNSS receivers. In Proceedings of the 19th International Technical Meeting of the Satellite Division of The Institute of Navigation (ION GNSS 2006), Fort Worth, TX, USA, 26–29 September 2006; pp. 790–798.
44. Tahir, M.; Presti, L.L.; Fantino, M. Characterizing different open loop fine frequency estimation methods for GNSS receivers. In Proceedings of the 2012 International Technical Meeting of The Institute of Navigation, Newport Beach, CA, USA, 30 January–1 February 2012; pp. 311–355.
45. Jin, T.; Yuan, H.; Ling, K.-V.; Qin, H.; Kang, J. Differential Kalman filter design for GNSS open loop tracking. *Remote Sens.* **2020**, *12*, 812. [CrossRef]
46. Wu, C.; Li, Y.; Luo, L.; Xie, J.; Wang, L. Two-step frequency estimation of GNSS signal in high-dynamic environment. *Int. J. Antennas Propag.* **2022**, *2022*, 1017206. [CrossRef]
47. Stienne, G.; Reboul, S.; Choquel, J.-B.; Benjelloun, M. Circular data processing tools applied to a phase open loop architecture for multi-channels signals tracking. In Proceedings of the 2012 IEEE/ION Position, Location and Navigation Symposium, Myrtle Beach, SC, USA, 23–26 April 2012; IEEE: Piscataway, NJ, USA, 2012; pp. 633–642.
48. Closas, P.; Fernández-Prades, C.; Fernández-Rubio, J.A. Maximum likelihood estimation of position in GNSS. *IEEE Signal Process. Lett.* **2007**, *14*, 359–362. [CrossRef]

49. Tahir, M.; Presti, L.L.; Fantino, M. A novel quasi-open loop architecture for GNSS carrier recovery systems. *Int. J. Navig. Obs.* **2012**, *2012*, 324858. [CrossRef]
50. Closas, P.; Fernandez-Prades, C.; Bernal, D.; Fernandez-Rubio, J.A. Bayesian direct position estimation. In Proceedings of the 21st International Technical Meeting of the Satellite Division of The Institute of Navigation (ION GNSS 2008), Savannah, GA, USA, 16–19 September 2008; pp. 183–190.
51. Closas, P.; Fernandez-Prades, C.; Fernandez-Rubio, J. A. Cramér–Rao bound analysis of positioning approaches in GNSS receivers. *IEEE Trans. Signal Process.* **2009**, *57*, 3775–3786. [CrossRef]
52. Closas, P.; Fernández-Prades, C. Bayesian nonlinear filters for direct position estimation. In Proceedings of the 2010 IEEE Aerospace Conference, Big Sky, MT, USA, 6–13 March 2010; IEEE: Piscataway, NJ, USA, 2010; pp. 1–12.
53. Closas, P.; Gusi-Amigo, A. Direct position estimation of GNSS receivers: Analyzing main results, architectures, enhancements, and challenges. *IEEE Signal Process. Mag.* **2017**, *34*, 72–84. [CrossRef]
54. Amar, A.; Weiss, A.J. New asymptotic results on two fundamental approaches to mobile terminal location. In Proceedings of the 2008 3rd International Symposium on Communications, Control and Signal Processing, St Julian's, Malta, 12–14 March 2008; IEEE: Piscataway, NJ, USA, 2008; pp. 1320–1323.
55. Ramesh Kumar, A. Direct Position Tracking in GPS Using Vector Correlator. Ph.D. Thesis, University of Illinois at Urbana-Champaign, Champaign, IL, USA, 2015.
56. Ng, Y. Improving the Robustness of GPS Direct Position Estimation. Ph.D. Thesis, University of Illinois at Urbana-Champaign, Champaign, IL, USA, 2016.
57. Chu, A.H.-P.; Chauhan, S.V.S.; Gao, G.X. GPS multireceiver direct position estimation for aerial applications. *IEEE Trans. Aerosp. Electron. Syst.* **2019**, *56*, 249–262. [CrossRef]
58. Alban, S.; Akos, D.M.; Rock, S.M. Performance analysis and architectures for INS-aided GPS tracking loops. In Proceedings of the 2003 National Technical Meeting of The Institute of Navigation, Anaheim, CA, USA, 22–24 January 2003; pp. 611–622.
59. Borio, D.; Sokolova, N.; Lachapelle, G. Memory discriminators for non-coherent integration in GNSS tracking loops. *Proc. European Navigation Conf. ENC* **2009**, *9*. Available online: https://api.semanticscholar.org/CorpusID:58704482 (accessed on 7 May 2025).
60. Borio, D.; Lachapelle, G. A non-coherent architecture for GNSS digital tracking loops. *Ann. Telecommun. Ann. Des TéLéCommunications* **2009**, *64*, 601–614. [CrossRef]
61. Xu, J. Beidou Satellite Navigation System Space Signal Interface Control Document Interpretation. *Int. Space* **2013**, 26–32. Available online: http://www.beidou.gov.cn/yw/xwzx/201712/W020171226734109234149.pdf (accessed on 7 May 2025).
62. Dunn, M.J.; Disl, D. *Global Positioning System Directorate Systems Engineering & Integration Interface Specification IS-GPS-200*; Global Positioning Systems Directorate: Los Angeles, CA, USA, 2012.
63. Chen, J. Research on Performance Enhancement Technology of Inertial Beidou Deep Integrated Navigation Under High Dynamic Conditions. Ph.D. Thesis, Nanjing University of Aeronautics and Astronautics, Nanjing, China, 2019.
64. Pany, T.; Riedl, B.; Winkel, J.; Wrz, T.; Jiménez-Baos, D. Coherent integration time: The longer, the better. *Inside GNSS* **2009**, *4*, 52–61.
65. Bernal, D.; Closas, P.; Fernandez-Rubio, J.A. Particle filtering algorithm for ultra-tight GNSS/INS integration. In Proceedings of the 21st International Technical Meeting of the Satellite Division of The Institute of Navigation (ION GNSS 2008), Savannah, Georgia, 16–19 September 2008; pp. 2137–2144.
66. Zhang, T.; Ban, Y.; Niu, X.; Guo, W.; Liu, J. Improving the design of MEMS INS-aided PLLs for GNSS carrier phase measurement under high dynamics. *Micromachines* **2017**, *8*, 135. [CrossRef]
67. Niu, X.; Ban, Y.; Zhang, Q.; Zhang, T.; Zhang, H.; Liu, J. Quantitative analysis to the impacts of IMU quality in GPS/INS deep integration. *Micromachines* **2015**, *6*, 1082–1099. [CrossRef]
68. Ren, T.; Petovello, M.G. A stand-alone approach for high-sensitivity GNSS receivers in signal-challenged environment. *IEEE Trans. Aerosp. Electron. Syst.* **2017**, *53*, 2438–2448. [CrossRef]
69. Lindsey, W.C.; Chie, C.M. Theory of oscillator instability based upon structure functions. *Proc. IEEE* **1976**, *64*, 1652–1666. [CrossRef]
70. Gaggero, P. *Effect of Oscillator Instability on GNSS Signal Integration Time*; University of Neuchtel: Neuchâtel, Switzerland, 2008.
71. Gowdayyanadoddi, N.S.; Broumandan, A.; Curran, J.T.; Lachapelle, G. Benefits of an ultra stable oscillator for long coherent integration. In Proceedings of the 27th International Technical Meeting of The Satellite Division of the Institute of Navigation (ION GNSS+ 2014), Denver, CO, USA, 11–15 September 2014; pp. 1578–1594.
72. Watson, R.; Lachapelle, G.; Klukas, R. Testing oscillator stability as a limiting factor in extreme high-sensitivity GPS applications. In Proceedings of the European Navigation Conference, Estoril, Portugal, 14–18 May 2006; Citeseer: Beijing, China, 2006; pp. 1–20.
73. Irsigler, M.; Eissfeller, B. PLL tracking performance in the presence of oscillator phase noise. *GPS Solut.* **2002**, *5*, 45–57. [CrossRef]

74. Pany, T.; Euler, H.-J.; Winkel, J. Indoor carrier phase tracking and positioning with difference correlators. In Proceedings of the 24th International Technical Meeting of the Satellite Division of The Institute of Navigation (ION GNSS 2011), Portland, OR, USA, 19–23 September 2011; pp. 2202–2213.
75. Pany, T.; Euler, H.; Winkel, J. Difference correlators. In *Does Indoor Carrier Phase Tracking Allow Indoor RTK*; 2012; pp. 62–73. Available online: https://www.academia.edu/3064-9765/1/1/10.20935/AcadMolBioGen7288 (accessed on 7 May 2025).
76. Li, Z. *Research on Deep Integration Technology for GNSS Carrier Phase Quality in Complex Signal Environment*; Wuhan University: Wuhan, China, 2019.
77. Zhodzishsky, M.; Kurynin, R.; Veitsel, A. A radical approach to reducing effects of quartz crystal oscillator instability on GNSS receiver performance. In Proceedings of the 2020 Systems of Signal Synchronization, Generating and Processing in Telecommunications (SYNCHROINFO), Svetlogorsk, Russia, 1–3 July 2020; IEEE: Piscataway, NJ, USA, 2020; pp. 1–18.
78. Borio, D.; Camoriano, L.; Presti, L.L.; Fantino, M. DTFT-based frequency lock loop for GNSS applications. *IEEE Trans. Aerosp. Electron. Syst.* **2008**, *44*, 595–612. [CrossRef]
79. Palmer, L. Coarse frequency estimation using the discrete Fourier transform (corresp.). *IEEE Trans. Inf. Theory* **1974**, *20*, 104–109. [CrossRef]
80. Yang, C. Tracking of GPS code phase and carrier frequency in the frequency domain. In Proceedings of the 16th International Technical Meeting of the Satellite Division of The Institute of Navigation (ION GPS/GNSS 2003), Fort Worth, TX, USA, 25–28 September 2003; pp. 628–637.
81. Schamus, J.J.; Tsui, J.B.; Lin, D.M. Real-time software GPS receiver. In Proceedings of the 15th International Technical Meeting of the Satellite Division of The Institute of Navigation (ION GPS 2002), Portland, Oregon, 24–27 September 2002; pp. 2561–2565.
82. Ba, X.; Liu, H.; Zheng, R.; Chen, J. A novel algorithm based on FFT for ultra high-sensitivity GPS tracking. In Proceedings of the 22nd International Technical Meeting of The Satellite Division of the Institute of Navigation (ION GNSS 2009), Savannah, GA, USA, 22–25 September 2009; pp. 1700–1706.
83. Yan, K.; Zhang, T.; Niu, X.; Zhang, H.; Zhang, P.; Liu, J. INS-aided tracking with FFT frequency discriminator for weak GPS signal under dynamic environments. *GPS Solut.* **2017**, *21*, 917–926. [CrossRef]
84. Wang, X.; Ji, X.; Feng, S.; Calmettes, V. A high-sensitivity GPS receiver carrier-tracking loop design for high-dynamic applications. *GPS Solut.* **2015**, *19*, 225–236. [CrossRef]
85. Jiang, R.; Wang, K.; Liu, S.; Li, Y. Performance analysis of a Kalman filter carrier phase tracking loop. *GPS Solut.* **2017**, *21*, 551–559. [CrossRef]
86. Liu, W.; Wu, L.; Hu, Y.; Huang, H.; Wang, S. GNSS/INS integrated navigation algorithm framework based on cascade vector tracking algorithm for USV. *Mar. Geod.* **2025**, *48*, 72–96. [CrossRef]
87. Kim, K.-H.; Jee, G.-I.; Song, J.-H. Carrier tracking loop using the adaptive two-stage Kalman filter for high dynamic situations. *Int. J. Control Autom. Syst.* **2008**, *6*, 948–953.
88. Yao, G.; Wu, W.; He, X. High dynamic carrier phase tracking based on adaptive Kalman filtering. In Proceedings of the 2011 Chinese Control and Decision Conference (CCDC), Mianyang, China, 23–25 May 2011; pp. 1245–1249.
89. Cheng, Y.; Chang, Q. A carrier tracking loop using adaptive strong tracking Kalman filter in GNSS receivers. *IEEE Commun. Lett.* **2020**, *24*, 2903–2907. [CrossRef]
90. Wang, Y.; Yang, R.; Morton, Y.J. Kalman filter-based robust closed-loop carrier tracking of airborne GNSS radio-occultation signals. *IEEE Trans. Aerosp. Electron. Syst.* **2020**, *56*, 3384–3393. [CrossRef]
91. Tang, X.; Falco, G.; Falletti, E.; Presti, L.L. Practical implementation and performance assessment of an extended Kalman filter-based signal tracking loop. In Proceedings of the 2013 International Conference on Localization and GNSS (ICL-GNSS), Turin, Italy, 5–27 June 2013; IEEE: Piscataway, NJ, USA, 2013; pp. 1–6.
92. Qin, H.; Liu, Y.; Jin, T. A novel adaptive EKF GNSS weak signal tracking algorithm. In Proceedings of the Conference on Navigation and Communication, Herndon, VA, USA, 11–13 May 2010.
93. Zeng, C.; Li, W. Application of extended Kalman filter for tracking high dynamic GPS signal. In Proceedings of the IEEE International Conference on Signal Processing, Zhuhai, China, 22–24 November 2016.
94. Psiaki, M.L.; Jung, H. Extended Kalman filter methods for tracking weak GPS signals. In Proceedings of the 15th International Technical Meeting of the Satellite Division of the Institute of Navigation (ION GPS 2002), Portland, OR, USA, 24–27 September 2002.
95. Jung, H.; Psiaki, M.L.; Powell, S.P. Kalman-filter-based semi-codeless tracking of weak dual-frequency GPS signals. In Proceedings of the 16th International Technical Meeting of the Satellite Division of The Institute of Navigation (ION GPS/GNSS 2003), Portland, OR, USA, 12 September 2003.
96. Zhu, Z.; Zhu, C.; Tang, G.; Li, S.; Huang, F. EKF based vector delay lock loop algorithm for GPS signal tracking. In Proceedings of the 2010 International Conference on Computer Design and Applications, Qinhuangdao, China, 25–27 June 2010.
97. Lashley, M.; Bevly, D.M.; Hung, J.Y. A valid comparison of vector and scalar tracking loops. In Proceedings of the IEEE/ION Position, Location and Navigation Symposium, Indian Wells, CA, USA, 4–6 May 2010; pp. 464–474.

98. Challa, S. *Fundamentals of Object Tracking*; Cambridge University Press: Cambridge, UK, 2011.
99. Bhattacharyya, S. *Performance and Integrity Analysis of the Vector Tracking Architecture of GNSS Receivers*; University of Minnesota: Minneapolis, MN, USA, 2012.
100. Lin, T.; O'Driscoll, C.; Lachapelle, G. Channel context detection and signal quality monitoring for vector-based tracking loops. In Proceedings of the 23rd International Technical Meeting of the Satellite Division of The Institute of Navigation (ION GNSS 2010), Portland, OR, USA, 21–24 September 2010; pp, 1875–1888.
101. Lashley, M.; Bevly, D.M. Comparison of traditional tracking loops and vector based tracking loops for weak GPS signals. In Proceedings of the 20th International Technical Meeting of the Satellite Division of the Institute of Navigation (ION GNSS 2007), Fort Worth, TX, USA, 25–28 September 2007; pp. 789–795.
102. Lashley, M.; Bevly, D.M. Comparison in the performance of the vector delay/frequency lock loop and equivalent scalar tracking loops in dense foliage and urban canyon. In Proceedings of the 24th International Technical Meeting of The Satellite Division of the Institute of Navigation (ION GNSS 2011), Portland, OR, USA, 19–23 September 2011; pp. 1786–1803.
103. Lin, H.; Xu, B.; Tang, X.; Ou, G. Performance analysis of signal tracking filter and navigation filter tight integration in GNSS receiver. In Proceedings of the 2016 5th International Conference on Computer Science and Network Technology (ICCSNT), Changchun, China, 10–11 December 2016; IEEE: Piscataway, NJ, USA, 2016; pp. 711–715.
104. Marçal, J.; Nunes, F. Robust vector tracking for GNSS carrier phase signals. In Proceedings of the 2016 International Conference on Localization and GNSS (ICL-GNSS), Barcelona, Spain, 28–30 June 2016; IEEE: Piscataway, NJ, USA, 2016; pp. 1–6.
105. Liu, J.; Cui, X.; Chen, Q.; Lu, M. Joint vector tracking loop in a GNSS receiver. In Proceedings of the 2011 International Technical Meeting of The Institute of Navigation, San Diego, CA, USA, 24–26 January 2011; pp. 1025–1032.
106. Jiang, C.; Chen, S.; Chen, Y.; Liu, D.; Bo, Y. GNSS vector tracking method using graph optimization. *IEEE Trans. Circuits Syst. II Express Briefs* **2020**, *68*, 1313–1317. [CrossRef]
107. Jiang, C.; Chen, Y.; Xu, B.; Jia, J.; Sun, H.; Chen, C.; Duan, Z.; Bo, Y.; Hyyppä, J. Vector tracking based on factor graph optimization for GNSS NLOS bias estimation and correction. *IEEE Internet Things J.* **2022**, *9*, 16209–16221. [CrossRef]
108. Zhang, X.; Li, H.; Yang, C.; Lu, M. Influence of spoofing interference on GNSS vector tracking loops. *J. Tsinghua Univ. (Sci. Technol.)* **2022**, *62*, 163–171. [CrossRef]
109. Liu, W.; Mou, M.; Gu, M.; Hu, Y.; Wang, S. A GNSS with FLL auxiliary PLL receiver vector tracking loop. *Mod. Electron. Technol.* **2022**, *45*, 1–5.
110. Lin, H.; Lou, S.; Tang, X.; Xu, B.; Ou, G. A vector and scalar hybrid tracking loop for new generation composite GNSS signal. In Proceedings of the China Satellite Navigation Conference (CSNC) 2017 Proceedings: Volume I, Shanghai, China, 23–25 May 2017; Springer: Berlin/Heidelberg, Germany, 2017; pp. 791–805.
111. Jiang, C.; Chen, Y.; Chen, C.; Hyyppä, J. Walking gait assisted vector tracking GNSS for pedestrian position. *IEEE Trans. Instrum. Meas.* **2023**, *72*, 1–11. [CrossRef]
112. Liu, D.; Xia, Q.; Jiang, C.; Wang, C.; Bo, Y. A LSTM-RNN-assisted vector tracking loop for signal outage bridging. *Int. J. Aerosp. Eng.* **2020**, *2020*, 2975489. [CrossRef]
113. Ni, S.; Li, S.; Xie, Y.; Deng, D. Overview of GNSS/INS ultra-tight integrated navigation. *J. Natl. Univ. Def. Technol.* **2023**, *45*, 48–59. [CrossRef]
114. Cox, D. Integration of GPS with inertial navigation systems (miscellaneous topics). *NAVIGATION J. Inst. Navig.* **1978**, *25*, 236–245. [CrossRef]
115. Gautier, J.D.; Parkinson, B.W. Using the GPS/INS generalized evaluation tool (GIGET) for the comparison of loosely coupled, tightly coupled and ultra-tightly coupled integrated navigation systems. In Proceedings of the 59th Annual Meeting of the Institute of Navigation and CIGTF 22nd Guidance Test Symposium (2003), Fairfax VA, USA, 23–25 June 2003; pp. 65–76.
116. Gustafson, D.; Dowdle, J. Deeply integrated code tracking: Comparative performance analysis. In Proceedings of the 16th International Technical Meeting of the Satellite Division of The Institute of Navigation (ION GPS/GNSS 2003), Fort Worth, TX, USA, 25–28 September 2003; pp. 2553–2561.
117. Edwards, W.L.; Clark, B.J.; Bevly, D.M. Implementation details of a deeply integrated GPS/INS software receiver. In Proceedings of the IEEE/ION Position, Location and Navigation Symposium, Indian Wells, CA, USA, 4–6 May 2010; IEEE: Piscataway, NJ, USA, 2010; pp. 1137–1146.
118. Niu, X.; Ban, Y.; Zhang, T.; Liu, J. Research progress and prospects of GNSS/INS deep integration. *Acta Aeronaut. Astronaut. Sin* **2016**, *37*, 2895–2908.
119. Ban, Y. *Research on the High Dynamic Tracking Technology of GNSS/INS Deep Integration*; Wuhan University: Wuhan, China, 2016.
120. Babu, R.; Wang, J. Ultra-tight GPS/INS/PL integration: A system concept and performance analysis. *GPS Solut.* **2009**, *13*, 75–82. [CrossRef]
121. Karaim, M.; Tamazin, M.; Noureldin, A. An efficient ultra-tight GPS/RISS integrated system for challenging navigation environments. *Appl. Sci.* **2020**, *10*, 3613. [CrossRef]

122. Yan, Z.; Ruotsalainen, L.; Gao, N.; Chen, X. Vector-tracking-based GNSS/INS deep coupling and experiment platform for urban scenarios. In Proceedings of the 2021 International Conference on Sensing, Measurement & Data Analytics in the Era of Artificial Intelligence (ICSMD), Xi'an, China, 15–17 October 2021; pp. 1–6. [CrossRef]
123. Yan, Z.; Chen, X.; Tang, X.; Zhu, X. Design and performance evaluation of the improved INS-assisted vector tracking for the multipath in urban canyons. *IEEE Trans. Instrum. Meas.* **2022**, *71*, 1–16. [CrossRef]
124. Yan, Z.; Ruotsalainen, L.; Chen, X.; Tang, X. An INS-assisted vector tracking receiver with multipath error estimation for dense urban canyons. *GPS Solut.* **2023**, *27*, 88. [CrossRef]
125. Gao, W.; Zhan, X.; Yang, R. INS-aiding information error modeling in GNSS/INS ultra-tight integration. *GPS Solut.* **2024**, *28*, 35. [CrossRef]
126. Abbott, A.S.; Lillo, W.E. Global Positioning Systems and Inertial Measuring Unit Ultratight Coupling Method. U.S. Patent 6,516,021, 4 February 2003.
127. Li, Z.; Zhang, L.; Chen, S.; Yang, C.; Ma, L. Overview and prospect of strapdown inertial/satellite ultra-compact integrated navigation technology. *Syst. Eng. Electron.* **2016**, *38*, 866–874.
128. Petovello, M.; Lachapelle, G. Comparison of vector-based software receiver implementations with application to ultra-tight GPS/INS integration. In Proceedings of the 19th International Technical Meeting of the Satellite Division of the Institute of Navigation (ION GNSS 2006), Dallas, TX, USA, 26–29 September 2006; pp. 1790–1799.
129. Jwo, D.-J.; Chung, F.-C. Fuzzy adaptive unscented Kalman filter for ultra-tight GPS/INS integration. In Proceedings of the 2010 International Symposium on Computational Intelligence and Design, Budapest, Hungary, 18–20 November 2010; IEEE: Piscataway, NJ, USA, 2010; Volume 2, pp. 229–235.
130. Jwo, D.-J.; Yang, C.-F.; Chuang, C.-H.; Lee, T.-Y. Performance enhancement for ultra-tight GPS/INS integration using a fuzzy adaptive strong tracking unscented Kalman filter. *Nonlinear Dyn.* **2013**, *73*, 377–395. [CrossRef]
131. Luo, Y.; Babu, R.; Wu, W.-Q.; He, X.-F. Double-filter model with modified Kalman filter for baseband signal pre-processing with application to ultra-tight GPS/INS integration. *GPS Solut.* **2012**, *16*, 463–476. [CrossRef]
132. Zhang, X.; Miao, L.; Shao, H. Tracking architecture based on dual-filter with state feedback and its application in ultra-tight GPS/INS integration. *Sensors* **2016**, *16*, 627. [CrossRef]
133. Xie, F.; Sun, R.; Kang, G.; Qian, W.; Zhao, J.; Zhang, L. A jamming tolerant BeiDou combined B1/B2 vector tracking algorithm for ultra-tightly coupled GNSS/INS systems. *Aerosp. Sci. Technol.* **2017**, *70*, 265–276. [CrossRef]
134. Li, Q.; Zhao, Y. An innovative high-precision scheme for a GPS/MEMS-SINS ultra-tight integrated system. *Sensors* **2019**, *19*, 2291. [CrossRef]
135. Liu, B.; Gao, Y.; Gao, Y.; Tong, K.; Wu, M. Non-consecutive GNSS signal tracking-based ultra-tight integration system of GNSS/INS for smart devices. *GPS Solut.* **2022**, *26*, 82. [CrossRef]
136. Cristodaro, C.; Falco, G.; Ruotsalainen, L.; Dovis, F. On the use of an ultra-tight integration for robust navigation in jammed scenarios. In Proceedings of the 32nd International Technical Meeting of the Satellite Division of The Institute of Navigation (ION GNSS+ 2019), Miami, FL, USA, 16–20 September 2019; pp. 2991–3004.
137. Coenen, A.; Van Nee, D. Novel fast GPS/GLONASS code-acquisition technique using low update rate FFT. *Electron. Lett.* **1992**, *28*, 863–865. [CrossRef]
138. Han, S.; Wang, W.; Chen, X.; Meng, W. Quasi-open-loop structure for high dynamic carrier tracking based on UKF. *Acta Aeronaut. Astronaut. Sin.* **2010**, *31*, 2393–2399.
139. Closas, P.; Fernández-Prades, C.; Fernández, A.; Wis, M.; Vecchione, G.; Zanier, F.; Garcia-Molina, J.A.; Crisci, M. Evaluation of GNSS direct position estimation in realistic multipath channels. In Proceedings of the 28th International Technical Meeting of the Satellite Division of The Institute of Navigation (ION GNSS+ 2015), Tampa, FL, USA, 14–18 September 2015; pp. 3693–3701.
140. Baker, B.; Givhan, A.; Martin, S. Performance evaluation of direct position estimation in high-dynamic GPS environments. In Proceedings of the ION 2024 Pacific PNT Meeting, Long Beach, CA, USA, 23–25 January 2024; pp. 406–416.
141. Huang, J.; Sun, R.; Yang, R.; Zhan, X.; Chen, W. Navigation domain multipath characterization using GNSS direct position estimation in urban canyon environment. In Proceedings of the 35th International Technical Meeting of the Satellite Division of The Institute of Navigation (ION GNSS+ 2022), Denver, CO, USA, 9–23 September 2022; pp. 2606–2617.
142. Vicenzo, S.; Xu, B.; Dey, A.; Hsu, L.-T. Experimental investigation of GNSS direct position estimation in densely urban area. In Proceedings of the 36th International Technical Meeting of the Satellite Division of The Institute of Navigation (ION GNSS+ 2023), Denver, CO, USA, 11–15 September 2023; pp. 2906–2919.
143. Jia, Q.; Guo, Q. Design of dual-mode DPE receiver based on GPS L1/BDS B1C signals. In Proceedings of the 2025 International Technical Meeting of The Institute of Navigation, Long Beach, CA, USA, 27–30 January 2025; pp. 928–936.
144. Ng, Y.; Gao, G.X. Direct position estimation utilizing non-line-of-sight (NLOS) GPS signals. In Proceedings of the 29th International Technical Meeting of the Satellite Division of The Institute of Navigation (ION GNSS+ 2016), Portland, OR, USA, 12–16 September 2016; pp. 1279–1284.

145. Ng, Y.; Gao, G.X. Mitigating jamming and meaconing attacks using direct GPS positioning. In Proceedings of the 2016 IEEE/ION Position, Location and Navigation Symposium (PLANS), Savannah, GA, USA, 11–14 April 2016; IEEE: Piscataway, NJ, USA, 2016; pp. 1021–1026.
146. Vicenzo, S.; Qi, X.; Xu, B.; Hsu, L.-T. Machine learning assisted GNSS direct position estimation for urban environments applications. In Proceedings of the 2024 International Technical Meeting of The Institute of Navigation, Long Beach, CA, USA, 23–25 January 2024; pp. 1129–1142.
147. Tang, S.; Li, H.; Closas, P. Single difference code-based technique for direct position estimation. In Proceedings of the 37th International Technical Meeting of the Satellite Division of The Institute of Navigation (ION GNSS+ 2024), Baltimore, MD, USA, 16–20 September 2024; pp. 2567–2575.

Disclaimer/Publisher's Note: The statements, opinions and data contained in all publications are solely those of the individual author(s) and contributor(s) and not of MDPI and/or the editor(s). MDPI and/or the editor(s) disclaim responsibility for any injury to people or property resulting from any ideas, methods, instructions or products referred to in the content.